AFCRL-69-0546

Technical Report 2183-4

AD707827

THE DYADIC DIFFRACTION COEFFICIENT FOR A PERFECTLY CONDUCTING WEDGE

P. H. Pathak and R. G. Kouyoumjian

The Ohio State University

ElectroScience Laboratory

Department of Electrical Engineering
Columbus, Ohio 43212

Contract Number AF19(628)-5929
Project No. 5635
Task No. 563502
Work Unit No. 56350201

Scientific Report No. 5

5 June 1970

Contract Monitor: John K. Schindler
Microwave Physics Laboratory

RECEIVED
JUN 30 1970
A

This document has been approved for public release and sale; its distribution is unlimited.

Air Force Cambridge Research Laboratories
Office of Aerospace Research
United States Air Force
Bedford, Massachusetts 01730

NOTICES

Qualified requestors may obtain additional copies from the Defense Documentation Center. All others should apply to the Clearinghouse for Federal Scientific and Technical Information.

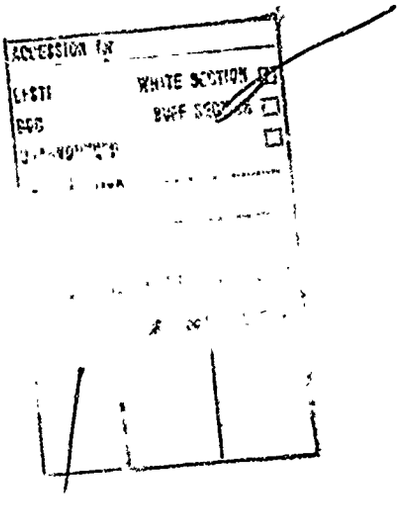

AFCRL-69-0546 Technical Report 2183-4

THE DYADIC DIFFRACTION COEFFICIENT FOR A PERFECTLY CONDUCTING WEDGE

P. H. Pathak and R. G. Kouyoumjian

Contract Number AF19(628)-5929
Project No. 5635
Task No. 563502
Work Unit No. 56350201

Scientific Report No. 5

5 June 1970

Contract Monitor: John K. Schindler
Microwave Physics Laboratory

This document has been approved for public release and sale; its distribution is unlimited.

Air Force Cambridge Research Laboratories
Office of Aerospace Research
United States Air Force
Bedford, Massachusetts 01730

FOREWORD

This report, OSURF Report Number 2183-4, was prepared by The ElectroScience Laboratory, Department of Electrical Engineering, The Ohio State University at Columbus, Ohio. Research was conducted under Contract AF 19(628)-5929. Dr. John K. Schindler, CRDG, of the Air Force Cambridge Research Laboratories at Bedford, Massachusetts was the Program Monitor for this research.

The material contained in this report is also used as a thesis submitted to the Department of Electrical Engineering, The Ohio State University as partial fulfillment for the degree Master of Science.

ABSTRACT

A ray-fixed coordinate system is introduced and used to derive a new, compact form of the dyadic diffraction coefficient for an electromagnetic wave incident on a perfectly-conducting wedge. This diffraction coefficient is merely the sum of two dyads; furthermore, with the use of simple correction factors which have the same form for plane, cylindrical, conical or spherical waves incident on the edge, the dyadic diffraction coefficient is valid in the transition regions of the shadow and reflection boundaries.

TABLE OF CONTENTS

BLANK PAGE

CHAPTER I
INTRODUCTION

The purpose of the research described in this report is to derive a dyadic diffraction coefficient for electromagnetic waves incident on a perfectly-conducting wedge. It is desired that this diffraction coefficient be valid, not only in the illuminated and shadowed regions surrounding the wedge, but also in the transition regions adjacent to the shadow and reflection boundaries. Furthermore, it is desired that the diffraction coefficient be compact and accurate so that it is useful for computational purposes. These objectives have been attained in the form of a new dyadic diffraction coefficient, which is derived in the pages to follow.

The diffraction coefficient is introduced in the geometrical theory of diffraction in order to relate the field of the ray incident at the edge to the field of edge-diffracted ray. The diffraction coefficient is analogous to the reflection coefficient used to relate incident and reflected fields. A description of the geometrical theory of diffraction is given in References 1, 2, 3. If the problem involves scalar waves, the diffraction coefficient is a scalar quantity; on the other hand, if the problem involves vector waves, as it does in the case of electromagnetic waves, the diffraction coefficient is a dyadic. The diffraction coefficient in question is found from an asymptotic solution of the pertinent wedge diffraction problem, where the result can be given a ray-optical interpretation. The diffraction by a wedge has received

a great deal of attention over the years, and some of the more important contributions to its asymptotic solution are described in the following paragraphs.

MacDonald[4] obtained an integral representation for the eigenfunction expansions of the total field. Plane, cylindrical and spherical wave illuminations of the wedge by scalar waves were treated. However, the earliest asymptotic solution to the wedge problem appears to have been due to Sommerfeld.[5] He considered the case of scalar plane wave illumination, and his solution is valid outside of the transition regions at the shadow and reflection boundaries; however, it is not valid within the transition regions. Pauli[6] and Oberhettinger[7] obtained uniform asymptotic solutions which can be used in the transition regions. Both of these solutions are restricted to the exterior wedge problem, i.e., they are restricted to wedge angles less than 180 degrees; furthermore, there is a deficiency in Pauli's solution that imposes a further limitation. This deficiency is pointed out in Reference 9. Felsen[8] has obtained uniform asymptotic solutions for plane, cylindrical and spherical wave illuminations of the wedge. His solutions can be applied to both the interior and exterior wedge problems. In addition to wedges with the usual Dirichlet and Neumann Boundary conditions, Felsen has considered wedges with impedance boundary conditions. Pauli obtained a factor type correction term which makes his solution valid in the transition region, whereas Oberhettinger and Felsen have additive type corrections. These differences result from the different methods used to treat

the pole close to the saddle point in the asymptotic solutions. Hutchins and Kouyoumjian[9,14] generalized Pauli's solution for the scalar plane wave illumination of the wedge and obtained a factor type correction for the transition regions, which makes the leading term in their asymptotic expansion more accurate than those of the solutions described previously. Their solution corrected the aforementioned deficiency in Pauli's solution. In addition, the relatively compact form of their solution further adds to its desirability from the computational point of view.

The work described thus far has been limited to the case of scalar waves. The more difficult vector diffraction problem has been treated by Nomura,[10] who obtained a uniform asymptotic solution for the problem of an oscillating electric dipole illuminating a perfectly-conducting wedge. Even though his solution employs a factor type correction for the transition region, the expressions for the field possess a rather complicated form and they are not amenable to easy computation. Tuzhilin[11,12] treated the scalar and vector wedge diffraction problems; his results possess additive type correction terms for the transition region which involve complicated integrals for the cylindrical and spherical wave illuminations. Recently Bowman and Senior[13] unified and simplified the results of Tuzhilin and others by treating the case of a conducting half-plane excited by an oscillating electric dipole. An asymptotic representation for the Hertz potential was presented with an additive type correction for the transition region. The results of Reference 13, although simpler than those of References 11 and 12 and

others, still lead to cumbersome expressions for the fields obtained from the space derivatives of the Hertz potential. In summary, none of the electromagnetic solutions described in References 10 through 13 appear to be in a form suitable for the derivation of a compact dyadic diffraction coefficient.

It was decided to derive the dyadic diffraction coefficient for several types of edge illumination. Although the diffraction coefficient is independent of the type of edge illumination outside of the transition regions, it differs with the type of edge illumination within the transition region. Let the edge of the wedge lie along the z-axis. In the case of plane and cylindrical waves incident on the perfectly-conducting wedge, the field components are readily found from E_z and H_z, the z-components of the electric and magnetic fields, respectively. In turn, the solutions for E_z and H_z reduce to the ordinary scalar diffraction problems. The incident spherical wave may have z-directed electric or magnetic current dipoles as its source. The electric and magnetic fields, due to these dipoles, can be obtained from F_z and A_z, the z-components of electric and magnetic vector potentials, respectively. Again, the solutions for A_z and F_z reduce to ordinary scalar diffraction problems.

In Chapter II asymptotic solutions of the scalar diffraction problems are obtained by the modified Pauli-Clemmow method of steepest descent. The wedge illuminated by a line source is treated first and an integral representation of the field is obtained from its eigenfunction expansion. By letting the line source recede to

infinity this integral representation is transformed into an integral representation for a plane wave incident on the wedge. The integral representation for the field of the point source illumination is deduced from the integral representation for the field of the line source illumination by a Fourier transformation involving the z-coordinate. After asymptotically evaluating these integrals, the scalar diffraction coefficients and their correction factors for the transition regions are obtained. These diffraction coefficients are of interest not only in the case of scalar diffraction, but also in the case of vector diffraction, where they appear in the dyadic diffraction coefficient.

In Chapter III the diffraction of electromagnetic waves by a perfectly-conducting wedge is treated. The plane and cylindrical wave solutions of Chapter II are generalized to oblique incidence, so that in the place of an incident cylindrical wave one has an incident conical wave whose source is a traveling wave electric or magnetic current line source. Starting with E_z and H_z one then determines integral representations for all of the field components. These integrals are then evaluated asymptotically.

In order to simplify the expression for the diffracted electromagnetic field, special coordinate systems for the incident and diffracted fields are introduced. These coordinate systems are suggested by the law of edge diffraction and they are fixed in the incident and diffracted rays. When the components of the incident and diffracted fields are written in this coordinate system, and

only the leading term in the asymptotic solution is retained, the resulting expression for the dyadic diffraction coefficient reduces to a sum of two dyads. If, instead, a simple edge-fixed coordinate system were used, the resulting dyadic diffraction coefficient would appear as a sum of seven dyads; thus, the importance of introducing the special ray-fixed coordinates can hardly be overemphasized.

The case of a spherical wave obliquely incident on a perfectly-conducting wedge is treated in a similar manner; in this case, the field components are found from A_z and F_z.

CHAPTER II
SCALAR WAVE DIFFRACTION

This chapter deals with the scalar wave diffraction by an impenetrable wedge; both Dirichlet and Neumann boundary conditions are treated. Plane wave, cylindrical wave and spherical wave illuminations of the edge are considered. The relationship of these problems to the electromagnetic problem is indicated.

A. Cylindrical Wave Illumination

Consider a z-directed, uniform line source of unit strength radiating cylindrical scalar waves in the presence of an impenetrable, infinite wedge as shown in Fig. 1. The total field, which consists of

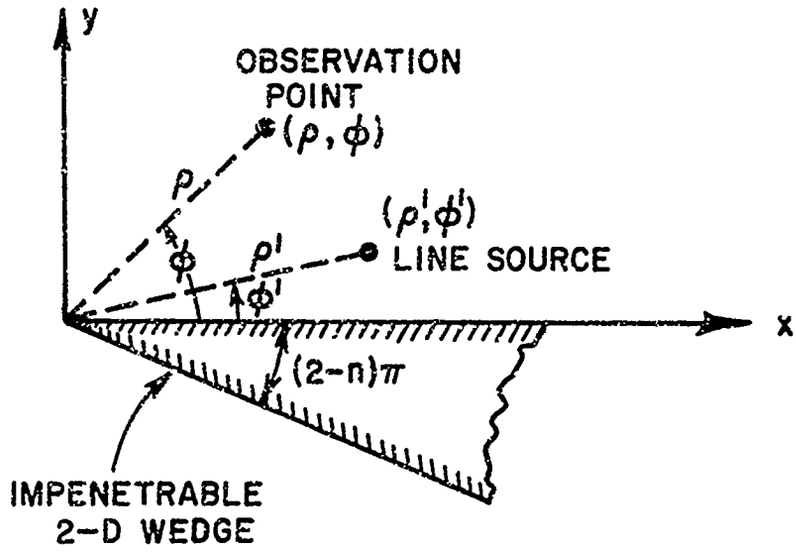

Fig. 1. The 2-D wedge and line source in the circular cylindrical coordinate system.

the incident and scattered components surrounding the wedge, is given by a two-dimensional scalar Green's function $G_{\substack{s \\ h}}(\bar{\rho},\bar{\rho}')$ where

$$(1) \qquad (\nabla_t^2 + k^2)\, G_{\substack{s \\ h}}(\bar{\rho},\bar{\rho}') = -\delta(|\bar{\rho} - \bar{\rho}'|)$$

∇_t^2 = the two-dimensional Laplacian operator in circular cylindrical coordinates, and $\delta(|\bar{\rho} - \bar{\rho}'|)$ is the Dirac Delta function. k = wave number of the linear, homogeneous and isotropic medium surrounding the wedge. $G_{\substack{s \\ h}}(\bar{\rho},\bar{\rho}')$ satisfies the following boundary conditions at the wedge surface:

$$(2) \qquad G_s(\bar{\rho},\bar{\rho}') = 0 \text{ at } \phi = 0,\ n\pi;$$

$$(3) \qquad \frac{\partial}{\partial\phi} G_h(\bar{\rho},\bar{\rho}') = 0 \text{ at } \phi = 0,\ n\pi.$$

Boundary condition (2) corresponds to the acoustic case for a soft wedge whereas (3) corresponds to the acoustic case for a hard wedge. In mathematical terminology, (2) corresponds to the homogeneous Dirichlet boundary condition and (3) corresponds to the homogeneous Neumann boundary condition.

Furthermore, $G_{\substack{s \\ h}}(\bar{\rho},\bar{\rho}')$ also satisfies the Sommerfeld radiation condition[15] and the Meixner edge condition,[16] respectively. Thus the solution for $G_{\substack{s \\ h}}(\bar{\rho},\bar{\rho}')$ is unique.

The above problem, depicted in Fig. 1, represents the basic canonical problem in this report. It will be used to deduce the solutions of the other canonical problems.

The Green's function $G_{\substack{s\\h}}(\bar{\rho},\bar{\rho}')$ for this canonical problem is given by a convergent eigenfunction expansion as

$$(4)\quad G_{\substack{s\\h}}(\bar{\rho},\bar{\rho}') = G_{\substack{s\\h}}(\rho,\phi;\rho',\phi') = \frac{-j}{4n}\sum_{m=0}^{\infty} \varepsilon_m J_{\frac{m}{n}}(k\rho)\, H^{(2)}_{\frac{m}{n}}(k\rho') \cdot \left[\cos\frac{m}{n}(\phi-\phi') \mp \cos\frac{m}{n}(\phi+\phi')\right],$$

where

$$0 \leq \phi,\ \phi' \leq n\pi$$

$$0 \leq \rho < \rho' < \infty\ ,$$

and

$$\varepsilon_m = 1,\ m = 0$$

$$= 2,\ m \neq 0.$$

$J_{\frac{m}{n}}(k\rho)$ and $H^{(2)}_{\frac{m}{n}}(k\rho')$ represent the cylindrical Bessel function of the first kind and the cylindrical Hankel function of the second kind, respectively. A time dependence of the $e^{+j\omega t}$ type is assumed and suppressed. $G_{\substack{s\\h}}$ represents the modal description of the waves existing in the presence of the wedge structure excited by a line source at (ρ',ϕ'). $G_{\substack{s\\h}}$ as given by (4) converges for all ρ,ϕ,ρ',ϕ' and n (interchanging ρ and ρ' in (4) yields $G_{\substack{s\\h}}$ for $\rho > \rho'$).

It is easy to see that the total electric field (z-directed) is proportional to G_s if the line source is electric, whereas the total magnetic field (z-directed) is proportional to G_h if the line source is magnetic. Thus, the scalar problem is useful in the treatment of the electromagnetic problem of a uniform electric or magnetic current line source illuminating a wedge which is perfectly conducting.

If the line source is electric, then the total electric field, E_z is given by

$$E_z(\bar{\rho}) = -j\omega\mu\, IG_s, \tag{5}$$

where ω is the angular frequency and μ is the permeability of the medium surrounding the wedge.

If the line source is magnetic, then the total magnetic field, H_z is given by

$$H_z(\bar{\rho}) = -j\omega\varepsilon\, MG_h, \tag{6}$$

where ε is the permittivity of the medium surrounding the wedge and I and M are the strengths of the electric and magnetic current line sources respectively.

An integral representation for the product, $J_{\frac{m}{n}}(k\rho)H^{(2)}_{\frac{m}{n}}(k\rho')$ is[4]

$$J_{\frac{m}{n}}(k\rho)H^{(2)}_{\frac{m}{n}}(k\rho') = -\frac{1}{\pi j}\int_0^{c-j\infty} e^{\frac{1}{2}[t-k^2(\rho^2+\rho'^2)t^{-1}]}\, I_{\frac{m}{n}}\left(\frac{k^2\rho\rho'}{t}\right)\frac{dt}{t} \tag{7}$$

$$c > 0,\ \frac{m}{n} > -1 \text{ and } |\rho| < |\rho'| .$$

$I_{\frac{m}{n}}(\frac{k^2\rho\rho'}{t})$ represents the modified cylindrical Bessel function of the first kind. A useful integral representation for $I_{\frac{m}{n}}(\frac{k^2\rho\rho'}{t})$ is given by[4]

$$I_{\frac{m}{n}}\left(\frac{k^2\rho\rho'}{t}\right) = -\frac{1}{2\pi}\int_{\gamma+j\infty}^{\gamma'+j\infty} e^{\frac{k^2\rho\rho'}{t}\cos\xi + j\frac{m}{n}\xi}\, d\xi, \tag{8}$$

where $-\pi < \gamma' < 0$,

$\pi < \gamma < 2\pi$.

Thus,

$$(9) \qquad I_{\frac{m}{n}}\left(\frac{k^2\rho\rho'}{t}\right) = -\frac{1}{2\pi}\int_{L} e^{\frac{k^2\rho\rho'}{t}\cos\xi + j\frac{m}{n}\xi}\, d\xi,$$

or

$$I_{\frac{m}{n}}\left(\frac{k^2\rho\rho'}{t}\right) = -\frac{1}{2\pi}\int_{L'} e^{\frac{k^2\rho\rho'}{t}\cos\xi - j\frac{m}{n}\xi}\, d\xi\ ,$$

where the contours L and L' are indicated in Fig. 2. Replacing the cosine terms in (4) by exponentials, and utilizing (7) and (9) in (4), interchanging the orders of summation and integrations, and choosing the L' contour representation for $I_0\left(\frac{k^2\rho\rho'}{t}\right)$ (corresponding to $m = 0$), allows one to write (4) as

$$(10) \qquad G_{\substack{s\\h}}(\bar{\rho},\bar{\rho}') = G(\bar{\rho},\bar{\rho}';\beta^-) \mp G(\bar{\rho},\bar{\rho}';\beta^+),$$

where

$$(11) \qquad G(\bar{\rho},\bar{\rho}';\beta^{\mp}) = -\frac{1}{8\pi^2 n}\int_0^{c-j\infty} e^{\frac{1}{2}[t-k^2(\rho^2+\rho'^2)t^{-1}]} \cdot$$

$$\cdot\left\{\int_L e^{\frac{k^2\rho\rho'}{t}\cos\xi}\left[\sum_{m=1}^{\infty} e^{j\frac{m}{n}(\xi+\beta^{\mp})}\right] d\xi + \right.$$

$$\left. + \int_{L'} e^{\frac{k^2\rho\rho'}{t}\cos\xi}\left[\sum_{m=0}^{\infty}{}' e^{-j\frac{m}{n}(\xi+\beta^{\mp})}\right] d\xi\right\}\frac{dt}{t}\ ,$$

and

$$(12) \qquad \beta^{\mp} \equiv \phi \mp \phi' = \beta$$

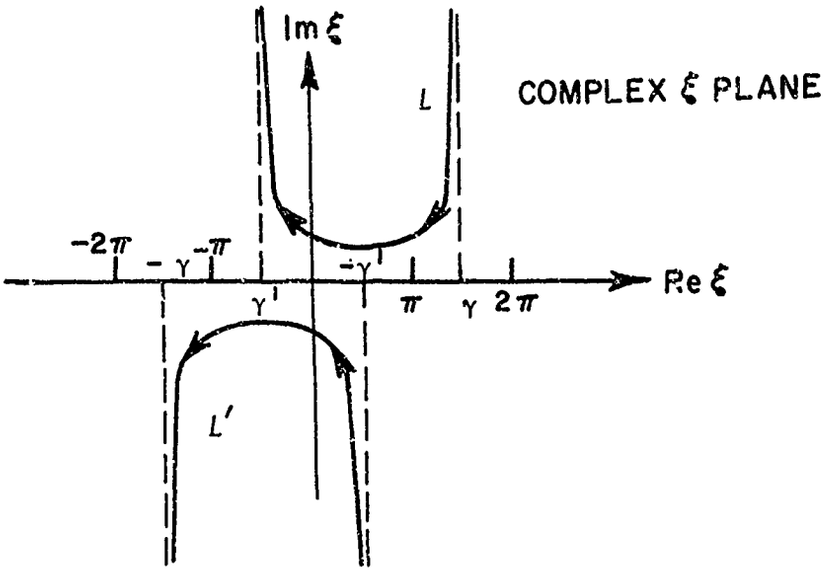

Fig. 2. The L and L' contours for the integral representation of $I_{\frac{m}{n}}(\frac{k^2\rho\rho'}{t})$ in the complex ξ plane.

Eq. (11) may be further simplified by noting that

$$
(13)\begin{cases}
\displaystyle\sum_{m=1}^{\infty} e^{j\frac{m}{n}(\xi+\beta)} = \sum_{m=0}^{\infty} e^{j\frac{m}{n}(\xi+\beta)} - 1, \\
\text{and} \\
\displaystyle\sum_{m=0}^{\infty} e^{\pm j\frac{m}{n}(\xi+\beta)} = \frac{1}{1 - e^{\pm j(\frac{\xi+\beta}{n})}} \quad . \\
\text{Also} \\
\displaystyle\sum_{m=0}^{\infty} e^{j\frac{m}{n}(\xi+\beta)} - 1 = -\frac{1}{2j}\cot\left(\frac{\xi+\beta}{2n}\right) - \frac{1}{2} \quad , \\
\text{and} \\
\displaystyle\sum_{m=0}^{\infty} e^{-j\frac{m}{n}(\xi+\beta)} = \frac{1}{2j}\cot\left(\frac{\xi+\beta}{2n}\right) + \frac{1}{2} \quad .
\end{cases}
$$

Therefore, (11) may be written via (13) as

$$(14)\qquad G(\rho,\rho';\beta) = -\frac{1}{8\pi^2 n}\int_0^{c-j\infty} e^{\frac{1}{2}[t-k^2(\rho^2+\rho'^2)t^{-1}]} \cdot$$

$$\cdot\left\{\int_L e^{\frac{k^2\rho\rho'}{t}\cos\xi}\left[-\frac{1}{2j}\cot\left(\frac{\xi+\beta}{2n}\right)-\frac{1}{2}\right]d\xi + \right.$$

$$\left. + \int_{L'} e^{\frac{k^2\rho\rho'}{t}\cos\xi}\left[\frac{1}{2j}\cot\left(\frac{\xi+\beta}{2n}\right)+\frac{1}{2}\right]d\xi\right\}\frac{dt}{t}\ ,$$

which on interchanging the orders of integration, gives

$$(15)\qquad G(\rho,\rho';\beta) = -\frac{1}{8\pi^2 n}\int_L d\xi\left\{-\frac{1}{2j}\cot\left(\frac{\xi+\beta}{2n}\right)-\frac{1}{2}\right\}\cdot$$

$$\cdot\left[\int_0^{c-j\infty}\frac{dt}{t}\ e^{\frac{1}{2}[t-k^2(\rho^2+\rho'^2)t^{-1}]+\frac{k^2\rho\rho'}{t}\cos\xi}\right] -$$

$$-\frac{1}{8\pi^2 n}\int_{L'} d\xi\left\{\frac{1}{2j}\cos\left(\frac{\xi+\beta}{2n}\right)+\frac{1}{2}\right\}\cdot$$

$$\cdot\left[\int_0^{c-j\infty}\frac{dt}{t}\ e^{\frac{1}{2}[t-k^2(\rho^2+\rho'^2)t^{-1}]+\frac{k^2\rho\rho'}{t}\cos\xi}\right]\ .$$

It can be shown that[4]

$$(16)\qquad -\frac{1}{2}\int_{c-j\infty}^{0} e^{\frac{t}{2}-\frac{z^2}{2t}}\ \frac{dt}{t} = K_0(jz),$$

where $K_0(jz)$ is the modified cylindrical Bessel function of the second kind, of order zero and argument, jz. Utilizing (16) in (15) gives

$$G(\rho,\rho';\beta) = -\frac{1}{4\pi^2 n}\int_{L} K_0(jk\sqrt{\rho^2+\rho'^2-2\rho\rho'\cos\xi})\left\{-\frac{1}{2j}\cot\left(\frac{\xi+\beta}{2n}\right)-\frac{1}{2}\right\}d\xi -$$

$$-\frac{1}{4\pi^2 n}\int_{L'} K_0(jk\sqrt{\rho^2+\rho'^2-2\rho\rho'\cos\xi})\left\{\frac{1}{2j}\cot\left(\frac{\xi+\beta}{2n}\right)+\frac{1}{2}\right\}d\xi ,$$

or, on combining terms one obtains

(17)

$$G(\rho,\rho';\beta) = \frac{1}{4\pi^2 n}\int_{L-L'} K_0(jk\sqrt{\rho^2+\rho'^2-2\rho\rho'\cos\xi})\cdot\left\{\frac{1}{2j}\cot\left(\frac{\xi+\beta}{2n}\right)+\frac{1}{2}\right\}d\xi .$$

Let $\quad k\sqrt{\rho^2+\rho'^2-2\rho\rho'\cos\xi} = z(\xi)$

then,

$$\frac{1}{4\pi^2 n}\int_{L-L'}\frac{1}{2}K_0(jz(\xi))d\xi = \left\{\int_{L}\frac{1}{2}K_0(jz(\xi))d\xi - \int_{L'}\frac{1}{2}K_0(jz(\xi))d\xi\right\}\cdot\frac{1}{4\pi^2 n}$$

$$= \frac{1}{8\pi^2 n}\left\{\int_{L}K_0(jz(\xi))d\xi - \int_{-L}K_0(jz(-\xi))d(-\xi)\right\} = 0,$$

since $z(\xi) = z(-\xi)$.

Finally, (17) can be written as

$$(18a)\quad G(\rho,\rho';\beta^{\mp}) = \frac{1}{4\pi^2 n}\int_{L-L'} d\xi\left\{\frac{1}{2j}\cot\left(\frac{\xi+\beta^{\pm}}{2n}\right)\right\}K_0(jk\sqrt{\rho^2+\rho'^2-2\rho\rho'\cos\xi}) .$$

Equation (18a) directly leads to a complex contour integral representation for $G_{\substack{s\\h}}(\bar{\rho},\bar{\rho}') = G(\rho,\rho';\beta^-) \mp G(\rho,\rho';\beta^+)$. The integral representation is still an exact form of the solution.

If $|z(\xi)|$ is large with respect to the order of $K_0(jz(\xi))$, one may use the large argument approximation

$$K_0(jz(\xi)) \sim \sqrt{\frac{\pi}{2jz(\xi)}}\, e^{-jz(\xi)}, \text{ where } z(\xi) = k\sqrt{\rho^2+\rho'^2-2\rho\rho' \cos \xi}$$

$$\text{and } -\pi \leq \arg (jz) \leq \pi.$$

In the asymptotic solution described later it will be seen that $|z|$ remains large in the neighborhood of the saddle points. Therefore, (18a) may be written as

$$(18b) \quad G(\rho,\rho';\beta^{\mp}) \approx \frac{1}{8\pi^2 jn} \int_{L-L'} d\xi \sqrt{\frac{\pi}{2jk(\rho^2+\rho'^2-2\rho\rho' \cos \xi)^{\frac{1}{2}}}} \cdot$$

$$\cdot \cot\left(\frac{\xi+\beta^{\mp}}{2n}\right) e^{-jk\sqrt{\rho^2+\rho'^2-2\rho\rho' \cos \xi}}.$$

Furthermore, the exponential may be approximated as

$$(19) \quad e^{-jk\sqrt{\rho^2+\rho'^2-2\rho\rho'\cos \xi}} = e^{-jk\sqrt{(\rho+\rho')^2-2\rho\rho'(\cos \xi + 1)}}$$

$$\approx e^{-jk(\rho+\rho') \{1 - \frac{\rho\rho'}{(\rho+\rho')^2}(1 + \cos \xi)\}}.$$

The above approximation will be justified a little later in the chapter.

Let

$$F_1(\xi,\beta^{\mp}) = \frac{1}{8\pi^2 jn} \sqrt{\frac{\pi}{2jk(\rho^2+\rho'^2-2\rho\rho' \cos \xi)^{\frac{1}{2}}}} \cot\left(\frac{\xi+\beta^{-}}{2n}\right) e^{-jk(\rho+\rho')}$$

and

$$f(\xi) = j\,[1 + \cos \xi] .$$

Thus,

$$(20) \qquad G(\bar{\rho},\bar{\rho}';\beta^{\mp}) \approx \int_{L-L'} d\xi\, F_1(\xi,\beta^{\mp})\, e^{\kappa f(\xi)}$$

is a compact notation for the expression in (18b) but containing the approximation of (19). $\kappa \equiv k\left(\frac{\rho\rho'}{\rho+\rho'}\right)$ and is assumed to be large. Thus, Eq. (20) is in the proper form for an asymptotic evaluation of the integral via the method of steepest descent. The steepest descent paths (SDP) selected for the asymptotic evaluation of (20) are those which pass through the saddle points of $f(\xi)$ at $\xi_s = \pm\pi$ for the following reason.

The saddle points of $f(\xi)$ occur at

$$\left.\frac{\partial f(\xi)}{\partial \xi}\right|_{\xi=\xi_s} = 0;$$

however $\xi_s = \pm\pi$ are the only ones chosen because the steepest descent paths through $\xi_s = \pm\pi$ allow one to close the $(L\text{-}L')$ contour, thereby facilitating the use of the Cauchy Residue Theorem. Figure 3 indicates the locations of the steepest descent paths through the pertinent saddle points at $\xi_s = \pm\pi$. It is easily seen that the required integral in (20) is given by:

$$(21) \quad \int_{L-L'} d\xi\, F_1(\xi,\beta^{\mp})\, e^{\kappa f(\xi)} d\xi = -\int_{SDP(\pi)} d\xi\, F_1(\xi,\beta^{\mp})\, e^{\kappa f(\xi)}\, d\xi -$$

$$- \int_{SDP(-\pi)} d\xi F_1(\xi,\beta^{\mp})\, e^{\kappa f(\xi)}\, d\xi +$$

$$+ 2\pi j \left[\begin{array}{l}\text{sum of the residues of } F_1(\xi,\beta^{\mp}) \text{ enclosed} \\ \text{between } L\text{-}L' \text{ and } SDP(\pm\pi)\end{array}\right] +$$

$$+ \text{(branch cut contributions, if any)} \quad .$$

The saddle points are the roots of

$$\left.\frac{df(\xi)}{d\xi}\right|_{\xi_s} = f'(\xi_s) = -j \sin \xi_s = 0.$$

Thus, it follows that

$$\xi_s = \pm \ell\pi, \text{ where } \ell = 0, 1, 2, 3, \cdots$$

As indicated earlier, only the case corresponding to $\ell = 1$ is of interest here.

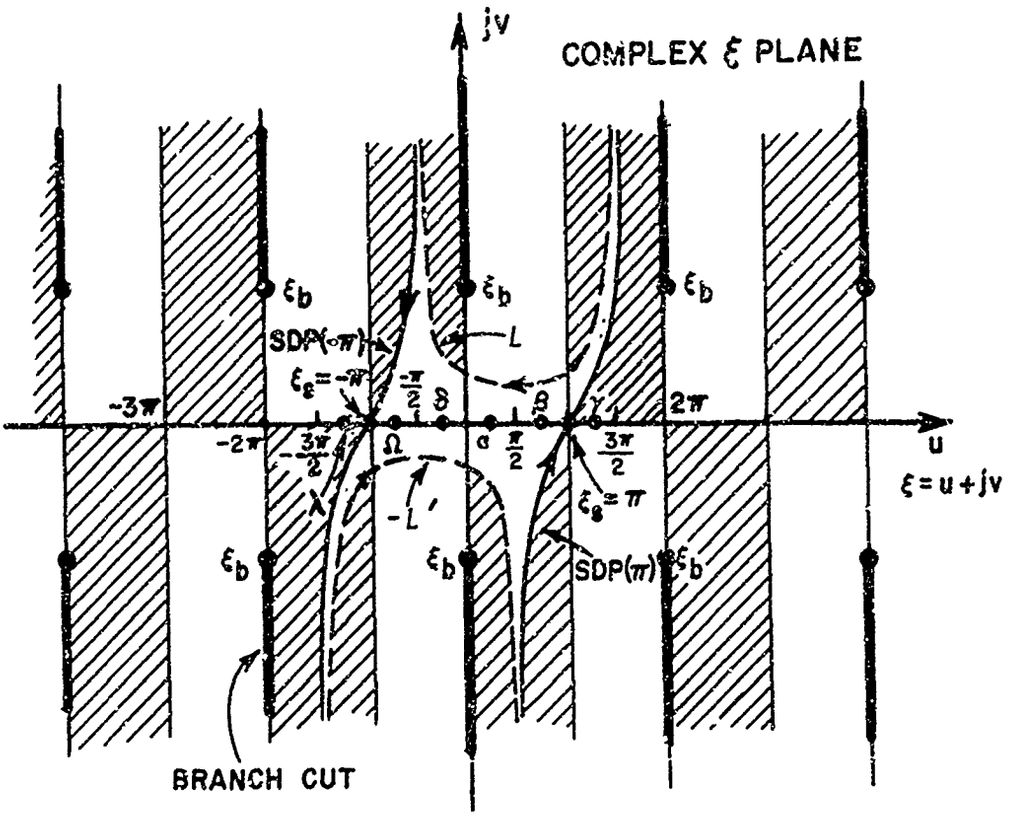

Fig. 3. Steepest descent paths (SDP±π) and the complex ξ plane topology.

In order to ensure convergence of the integral in (18b), one must have Re $f(\xi) < 0$ as $|\text{Im } \xi| \to \infty$. The portions of the complex ξ plane for which Re $f(\xi) < 0$ as $|\text{Im } \xi| \to \infty$ are shown as shaded vertical strips in Fig. 3. The SDP equations are found from the condition that

$$\text{Im } f(\xi) = \text{Im } f(\xi_s)$$

or

$$\cos u \cosh v = -1, \text{ where } \xi = u + jv.$$

The above equation is valid for $\xi_s = \pm\pi$ and the paths chosen are depicted in Fig. 3, the choice, as mentioned before, being governed by the fact that Re $f(\xi) < 0$ on the SDP($\pm\pi$) as $|\text{Im } \xi| \to \infty$ (where Im $\xi \equiv v$), and that these paths blend in with the $L - L'$ contours as $|\text{Im } \xi| \to \infty$, thereby allowing one to obtain a closed path of integration. (The paths corresponding to the images of SDP($\pm\pi$) about Re $\xi = \pm\pi$ also satisfy cos u cosh v = -1 but are paths for which Re $f(\xi) > 0$ as $|\text{Im } \xi| \to \infty$).

It is desirable at this juncture, to study the singularities of $F_1(\xi,\beta^{\pm})$ in the complex ξ plane.

$$F_1(\xi,\beta^{\mp}) = \frac{1}{8\pi^2 jn}\sqrt{\frac{\pi}{2jk(\rho^2+\rho'^2-2\rho\rho'\cos\xi)^{\frac{1}{2}}}}\cot\left(\frac{\xi+\beta^{\mp}}{2n}\right)e^{-jk(\rho+\rho')}.$$

$F_1(\xi,\beta^{\pm})$ has branch point singularities at $\xi = \xi_b$ which are the roots of

$$\rho^2 + \rho'^2 - 2\rho\rho' \cos \xi_b = 0$$

For the case where $\rho \neq \rho'$, it follows that $\rho^2 + \rho'^2 > 2\rho\rho'$, and therefore

$$\xi_b = 2\ell\pi \pm j \cosh^{-1} \frac{\rho^2 + \rho'^2}{2\rho\rho'} \quad , \text{where } \ell = 0, \pm 1, \pm 2, \cdots$$

The branch points and the branch cut locations are indicated in Fig. 3, where it is seen that the branch points are not in the vicinity of the saddle points at $\xi_s = \pm\pi$, and the branch cuts lie outside the closed path formed by $L - L'$ and SDP($\pm\pi$), so that the closed path is unaffected by the branch cuts. The integrand is single valued on and within the closed path, and since no deformations of this path are necessary for single valuedness, the branch cut does not contribute to the integral.

The pole type singularities of $F_1(\xi)$ occur at $\xi = \xi_p$, where ξ_p are specified by

$$\xi_p = -\beta^{\mp} + 2nN\pi, \quad N = 0, \pm 1, \pm 2, \cdots$$

The residues corresponding to ξ_p are evaluated for $|\xi_p| \leq \pi$ as only these poles lie within the closed path of integration since $\beta^{\mp} \equiv \phi \mp \phi'$, (it is easily seen that ξ_p is a real quantity). It can be shown that ξ_p are simple poles.

For sufficiently large κ, the major contribution to the integrals evaluated over SDP ($\pm\pi$) occurs only from the "immediate vicinity" of the saddle points ($\xi_s = \pm\pi$); hence it follows that the approximation of (19) is justified, as $|(1 + \cos \xi)|$ is small for $\xi \approx \xi_s$.

The first order saddle point approximation for a pole not close to the saddle point is given by

$$(22)\qquad \int_{SDP(\pm\pi)} F_1(\xi,\beta^{\mp})e^{\kappa f(\xi)}d\xi \sim F_1(\pm\pi,\beta^{\mp})\, e^{\kappa f(\pm\pi)}\left|\sqrt{\frac{-2\pi}{\kappa f''(\pm\pi)}}\right| e^{j\{\frac{\pi}{4}_{-3\pi/4}\}}$$

in which $e^{j\frac{\pi}{4}}$ is associated with $\xi_s = \pi$, and $e^{j\left(\frac{-3\pi}{4}\right)}$ with $\xi_s = -\pi$.

The residue contribution to the integral over the closed path, c is given by

$$\oint_c F_1(\xi,\beta^{\mp})e^{\kappa f(\xi)}d\xi = \oint_c \frac{P(\xi,\beta^{\mp})}{Q(\xi,\beta^{\mp})}d\xi = 2\pi j \sum_p \left[\frac{P(\xi_p,\beta^{\mp})}{Q'(\xi_p,\beta^{\mp})}\right],$$

where $c = (L - L') + SDP(\pi) + SDP(-\pi)$, and $P(\xi,\beta^{\mp})$ and $Q(\xi,\beta^{\mp})$ are both analytic functions of the complex variable, ξ.

$$P(\xi,\beta^{\mp}) = \sqrt{\frac{\pi}{2jk(\rho^2+\rho'^2-2\rho\rho'\cos\xi)^{\frac{1}{2}}}}\cos\left(\frac{\xi+\beta^{\mp}}{2n}\right)\, e^{-jk\sqrt{\rho^2+\rho'^2-2\rho\rho'\cos\xi}}$$

and

$$Q(\xi,\beta^{\mp}) = 8\pi^2 jn \sin\left(\frac{\xi+\beta^{\mp}}{2n}\right)$$

with

$$Q'(\xi,\beta^{\mp}) = 4\pi^2 j \cos\left(\frac{\xi+\beta^{\mp}}{2n}\right) .$$

The residue at $\xi_p = -\beta^{\mp} + 2nN\pi$ is thus given by

$$(23)\qquad \frac{1}{2\pi j}\left\{-\frac{j}{4}\sqrt{\frac{2j}{\pi k(\rho^2+\rho'^2-2\rho\rho'\cos[-\beta^{\mp}+2nN\pi])^{\frac{1}{2}}}}\cdot e^{-jk\sqrt{\rho^2+\rho'^2-2\rho\rho'\cos[-\beta^{\mp}+2nN\pi]}}\right\} U[\pi-|-\beta^{\mp}+2nN\pi|],$$

which may be recognized as the asymptotic form of

$$\frac{1}{2\pi j}\left\{-\frac{j}{4}H_0^{(2)}(k\sqrt{\rho^2+\rho'^2-2\rho\rho'\cos[-\beta^{\mp}+2nN\pi]})\right\}\ U[\pi-|-\beta^{\mp}+2nN\pi|],$$

and therefore represents the geometrical optics contribution in terms of the line source fields due to the source or it's image (the total geometrical optics contribution being a superposition of the incident and the reflected fields).

$$U(t) = \begin{cases} 0, & \text{if } t < 0 \\ \frac{1}{2}, & \text{if } t = 0 \\ 1, & \text{if } t > 0. \end{cases}$$

$U(0) = \frac{1}{2}$ ensures the Cauchy principal value when the pole singularity lies on the closed contour c. The function $U(\pi-|-\beta^{\mp}+2nN\pi|)$ automatically restricts the geometrical optics contributions to aspects defined by $|-\beta^{\mp} + 2nN\pi| \leq \pi$, so that the contributions from poles outside the closed contour, c, are not included.

Thus, for the $N = 0$ case, one obtains for the geometrical optics contribution, $G_{\substack{s\\h}}^{g.o.}$ the following field

$$(24)\quad G_{\substack{s\\h}}^{g.o.} \sim \left\{-\frac{j}{4}\sqrt{\frac{2j}{\pi k(\rho^2+\rho'^2-2\rho\rho'\cos(\phi-\phi'))^{\frac{1}{2}}}}\ \cdot\right.$$

$$\left.\cdot\ e^{-jk(\rho^2+\rho'^2-2\rho\rho'\cos(\phi-\phi'))^{\frac{1}{2}}}\ U(\pi-|\phi-\phi'|)\right\}\ \mp$$

$$\mp\left\{-\frac{j}{4}\sqrt{\frac{2j}{\pi k(\rho^2+\rho'^2-2\rho\rho'\cos(\phi+\phi'))^{\frac{1}{2}}}}\ \cdot\right.$$

$$\left.\cdot\ e^{-jk(\rho^2+\rho'^2-2\rho\rho'\cos(\phi+\phi'))^{\frac{1}{2}}}\ U(\pi-|\phi+\phi'|)\right\}.$$

(The minus (plus) sign between the two terms on RHS of (24) corresponds to the soft (hard) boundary condition). The first term on the right of (24) is the direct source (at ρ',ϕ') radiation at the observation point (at ρ,ϕ), whereas the second term represents the reflected wave contribution at the observation point (at ρ,ϕ) which appears to emanate from a virtual line source (at $\rho',-\phi'$). The reflection occurs from the wedge face, $\phi = 0$. In general, the incident field is described by $N = 0$ and $\beta^- = \phi-\phi'$. The reflected field from the surface $\phi = 0$, resulting from the incident field, is described by $N = 0$ and $\beta^+ = \phi + \phi'$. Other values of N describe fields which may be reflected either from the surface $\phi = 0$ or the surfaces $\phi = n\pi$.

Since the total field is composed of the geometrical optics field and the diffracted field, it follows that the saddle point contributions must yield the diffracted ray field in accordance with Keller's theory. The first order saddle point results for large $(k\rho\rho')/(\rho+\rho')$ as obtained from (22) is given as

$$G_{s,h}^{d} = -\left\{\left[\int_{SDP(\pi)} F_1(\xi,\beta^-)e^{\kappa f(\xi,\beta^-)}d\xi + \int_{SDP(-\pi)} F_1(\xi,\beta^-)e^{\kappa f(\xi,\beta^-)}d\xi\right] \mp \left[\int_{SDP(\pi)} F_1(\xi,\beta^+)e^{\kappa f(\xi,\beta^+)}d\xi + \int_{SDP(-\pi)} F_1(\xi,\beta^+)e^{\kappa f(\xi,\beta^+)}d\xi\right]\right\},$$

or,

$$G_{s,h}^{d} \sim \frac{e^{-jk(\rho+\rho')}}{8\pi nk\sqrt{\rho\rho'}}\left\{\left[e^{j\frac{\pi}{2}}\cot\left(\frac{\beta^-+\pi}{2n}\right) + e^{-j\frac{\pi}{2}}\cot\left(\frac{\beta^--\pi}{2n}\right)\right] \mp \left[e^{j\frac{\pi}{2}}\cot\left(\frac{\beta^++\pi}{2n}\right) + e^{-j\frac{\pi}{2}}\cot\left(\frac{\beta^+-\pi}{2n}\right)\right]\right\},$$

i.e.,

$$(25)\qquad G_{\substack{s\\h}}^{d} \sim \frac{1}{4\pi jk}\frac{e^{-jk(\rho+\rho')}}{\sqrt{\rho\rho'}}\left\{\frac{\frac{1}{n}\sin\frac{\pi}{n}}{\cos\frac{\pi}{n}-\cos\frac{\beta^-}{n}} \mp \frac{\frac{1}{n}\sin\frac{\pi}{n}}{\cos\frac{\pi}{n}-\cos\frac{\beta^+}{n}}\right\}.$$

For N = 0 case, the total field surrounding the wedge is given asymptotically by superposing the results of (24) and (25) as indicated by (21).

The value of the incident wave at the edge is given by, u^i where

$$u^i = -\frac{j}{4}H_o^{(2)}(k\rho') \sim -\frac{j}{4}\sqrt{\frac{2j}{\pi k\rho'}}\; e^{-jk\rho'},$$

for large $k\rho'$. Therefore, in accordance with the geometrical theory of diffraction, $G_{\substack{s\\h}}^{d}$ may be written as

$$(26)\qquad G_{\substack{s\\h}}^{d} \sim \left[u^i \sim -\frac{j}{4}\sqrt{\frac{2j}{\pi k\rho'}}\,e^{-jk\rho'}\right] \quad D_{\substack{s\\h}} \quad \frac{e^{-jk\rho}}{\sqrt{\rho}},$$

for large $k\rho\rho'/(\rho+\rho')$, where $D_{\substack{s\\h}}$ is the wedge diffraction coefficient associated with either the soft or the hard boundary condition at the wedge surface. The factor $\frac{e^{-jk\rho}}{\sqrt{\rho}}$ describes the variation of the amplitude and phase of the field of the diffracted rays emanating from the edge and traveling in the positive $\hat{\rho}$ direction. Comparing (25) with (26) it is seen that

$$(27)\qquad D_{\substack{s\\h}} = \frac{e^{-j\pi/4}}{\sqrt{2\pi k}}\left[\frac{\frac{1}{n}\sin\frac{\pi}{n}}{\cos\frac{\pi}{n}-\cos\left(\frac{\phi-\phi'}{n}\right)} \mp \frac{\frac{1}{n}\sin\frac{\pi}{n}}{\cos\frac{\pi}{n}-\cos\left(\frac{\phi+\phi'}{n}\right)}\right].$$

The result indicated in (27) is identical to that deduced by Sommerfeld.[5] This result fails at the shadow and reflection boundaries where $\frac{\phi\pm\phi'}{n} = \frac{\pi}{n} + 2N\pi$, and it is evident that at the shadow and

reflection boundaries the diffraction coefficient becomes singular.

As mentioned earlier, $\phi = \phi' + \pi$ (N=0) defines the shadow boundary; however a shadow boundary does not occur if the exterior wedge angle $n\pi < \pi$ or if $n\pi - \pi < \phi' < \pi$ in the case where $n\pi - \pi > 0$. A reflection boundary associated with the wedge surface $\phi = 0$ occurs at $\phi = \pi - \phi'$ (N=0); if $n\pi > \pi - \phi'$. Other reflection boundaries may result from the reflections at the two surfaces.

In the transition regions of the shadow or a reflection boundary a pole is close to the saddle point. Later, we will be interested in the pole closest to the π saddle point, and the pole closest to the $-\pi$ saddle point. The values of N associated with these poles are defined to be N^+ and N^-, respectively. The value of $N^\pm$ is decided by the integer which most nearly satisfies the equation:

$$2nN^{\pm}\pi - \beta = \pm\pi \ ,$$

where $$\beta = \beta^{\mp} \equiv \phi \mp \phi' .$$

Whenever the poles of the geometrical optics fields lie in the vicinity of the saddle points which happens when the observation point is in the transition region, the ordinary steepest descent method is not applicable and a more sophisticated approach is necessary. This approach accounts for the pole singularity of $F_1(\xi)$ when it is in the vicinity of the saddle points of $f(\xi)$; and this method will be referred to as the "Pauli-Clemmow modification of the method of steepest descent".[9,14,17] This modified steepest descent method has been presented for a general case with sufficient details in Appendix I. Hence, no formal derivations will be presented for

the different problems corresponding to the different source illuminations considered in this report. Only the results will be presented for the sake of brevity. A summary of the details in Appendix I may be stated in the following manner.

The modified steepest descent method essentially involves replacing the integrand by a product of two functions, one of which is singular with a simple pole and describes the effect of the pole near the saddle point in question; the other factor is analytic in the neighborhood of the pole and the saddle point in question. The analytic portion of the integrand is then expanded in a MacLaurin series about the saddle point and the resulting series is integrated termwise. In all of the results presented in this report, only the first term of the MacLaurin expansion is retained for simplicity. Thus, the results presented here correspond to a first order asymptotic approximation. Equation (25) is corrected through the modified steepest descent method of Appendix I, from where $G_{\substack{s\\h}}^{d}$ (diffracted fields) for large $\kappa = (k\rho\rho')/(\rho+\rho')$ is directly given by

$$(28)\quad G_{\substack{s\\h}}^{d} \sim -\frac{e^{-jk(\rho+\rho')}}{8\pi^2 jn}\sqrt{\frac{\pi}{2jk(\rho+\rho')}}\;\sqrt{\frac{2\pi(\rho+\rho')}{\kappa\rho\rho'}}\left[\left\{e^{j\frac{\pi}{4}}\cot\left(\frac{\pi+\beta^-}{2n}\right)F[\kappa a^+(\beta^-)]-\right.\right.$$
$$\left.-e^{-j\frac{3\pi}{4}}\cot\left(\frac{\pi-\beta^-}{2n}\right)\;F[\kappa a^-(\beta^-)]\right\}\mp\left\{e^{j\frac{\pi}{4}}\cot\left(\frac{\pi+\beta^+}{2n}\right)\;F[\kappa a^+(\beta^+)]-$$
$$\left.\left.-e^{-j\frac{3\pi}{4}}\cot\left(\frac{\pi-\beta^+}{2n}\right)\;F[\kappa a^-(\beta^+)]\right\}\right]\;.$$

(Note: $\beta^{\mp} \equiv \phi \mp \phi'$). As before, $G_{\substack{s\\h}}^{d}$ may be re-expressed for interpretation in terms of the GTD as follows.

$$(29) \qquad G_{\substack{s\\h}}^{d} \sim \left[u^{i} \sim \frac{-j}{4}\sqrt{\frac{2j}{\pi k\rho'}}\, e^{-j\, k\rho'}\right] \quad D_{\substack{s\\h}} \quad \frac{e^{-jk\rho}}{\sqrt{\rho}} \ ,$$

where, u^{i} represents the line source field incident at the edge. The new diffraction coefficient, denoted by $D_{\substack{s\\h}}$ is given as

$$(30) \qquad D_{\substack{s\\h}} = \{d^{+}(\beta^{-},n)\ F[\kappa a^{+}(\beta^{-})] + d^{-}(\beta^{-},n)\ F\ \kappa a^{-}(\beta^{-})]\} \ \mp$$

$$\mp \{d^{+}(\beta^{+},n)\ F[\kappa a^{+}(\beta^{+})] + d^{-}(\beta^{+},n)\ F[\kappa a^{-}(\beta^{+})]\} \ ,$$

where

$$(31) \qquad d^{\pm}(\beta,n) \equiv -\frac{e^{-j\frac{\pi}{4}}}{n\sqrt{2\pi k}} \quad \frac{1}{2}\cot\left(\frac{\pi\pm\beta}{2n}\right) \ ,$$

$$\beta = \beta^{\mp} \equiv \phi \mp \phi', \quad \kappa = k\rho\rho'/(\rho+\rho')$$

and

$$(32) \qquad F[\kappa a^{\pm}(\beta)] = 2j\sqrt{\kappa a^{\pm}(\beta)}\ e^{j\kappa a^{\pm}(\beta)} \int_{\sqrt{\kappa a^{\pm}(\beta)}}^{\infty} e^{-j\tau^{2}}\, d\tau,$$

where the positive branch of the square root is taken, and

$$(33) \qquad a^{\pm}(\beta) = \{1 + \cos(-\beta + 2nN^{\pm}\pi)\} \ .$$

(The superscript + (or -) refers to the saddle point at $\zeta_s = +\pi$ (or $\xi_s = -\pi$).)

It can be shown that for $\kappa a^{\pm}(\beta) > 10$ Eq. (30) reduces to Eq. (27). This is due to the fact that $F[\kappa a^{\pm}(\beta)] \to 1$ as $\kappa a^{\pm}(\beta) \to \infty$,

but for practical purposes $ka^{\pm}(\beta) > 10$ is a sufficient condition to replace the F factor by unity.

The result of (28) or (29) yields a uniformly asymptotic representation for the total field so that the diffracted field properly compensates for the discontinuity in the geometrical optics fields across the transition boundaries, thereby yielding a total field (geometrical optics plus the diffracted fields) which is continuous everywhere. This can be verified by taking the limit of Eq. (28) or (29) as one approaches the transition boundaries from either side. Further, the total field obtained via the limiting process on either side of the boundary exactly equals the "Cauchy principal value" resulting from $U(0) \equiv \frac{1}{2}$, as explained earlier, i.e., the Cauchy principal value yields one half the residue contribution associated with the pole corresponding to geometrical optics incident (or reflected) wave when it happens to fall exactly on the saddle point in question thereby defining the total field on the shadow (or reflection) boundary. This continuity of fields at the shadow and reflection boundaries will be described in the following paragraph.

It may be easily verified that the diffracted field just within the lit side ($\phi-\phi' = \pi-\varepsilon$; $\varepsilon>0$) of the shadow boundary gives in the limit ($\varepsilon\to 0$) the following:

$$(34) \qquad -\frac{1}{2}\left\{\frac{-j}{4}\sqrt{\frac{2}{\pi k(\rho+\rho')}}\; e^{-j[k(\rho+\rho')-\pi/4]}\right\} ,$$

whereas the diffracted field just within the dark side of the shadow boundary ($\phi-\phi' = \pi+\varepsilon$, $\varepsilon>0$) yields in the limit ($\varepsilon\to 0$) the following:

(35) $$\frac{1}{2}\left\{-\frac{j}{4}\sqrt{\frac{2}{\pi k(\rho+\rho')}}\ e^{-j[k(\rho+\rho')-\pi/4]}\right\} .$$

The incident ray field which is visible just within the lit side ($\phi-\phi' = \pi-\varepsilon$; as $\varepsilon\to 0$ and $\varepsilon>0$) of the shadow boundary is

(36) $$\left\{-\frac{j}{4}\sqrt{\frac{2}{\pi k(\rho+\rho')}}\ e^{-j[k(\rho+\rho')-\pi/4]}\right\} .$$

(Equation (36) is just the large argument approximation for the line source field, $-j/4\ H_0^{(2)}[k(\rho+\rho')]$). The total field just within the lit side on the shadow boundary is given by the sum of the results of (34) and (36) and it is seen to equal the total field just within the dark side of the shadow boundary given by (35). Thus, the total field is continuous across the shadow boundary and equals one half* the geometrical optics incident ray field, which as indicated earlier is exactly the Cauchy principal value associated with the incident wave pole for the shadow boundary, and is given by

(37) $$\frac{1}{2}\left\{-\frac{j}{4}\sqrt{\frac{2}{\pi k(\rho+\rho')}}\ e^{-j[k(\rho+\rho')-\pi/4]}\right\} .$$

Similarly, the total "scattered" field on the reflection boundary is one half* the geometrical optics field of the reflected ray (just within the reflection boundary). The incident ray field is of course continuous across the reflection boundary. The total field (incident plus scattered) is thus continuous across the reflection boundary.

It is of interest to note that the solution presented above for the canonical problem involving a perfectly conducting wedge excited by a line source (electric or magnetic) is the same as

*In this discussion $k\rho\rho'/\rho+\rho'$ is assumed to be large.

that conjectured by Rudduck and Tsai[18] except that the results of Reference 18 employ the Pauli result for the plane wave diffraction coefficient instead of the generalized Pauli result given in References 9 and 14.

B. Plane Wave Illumination

The plane wave incidence case is treated in this section. The result for the plane wave case may be obtained by letting $\rho' \to \infty$ in the line source case of Section A so that $k\rho\rho'/(\rho+\rho') \to k\rho$ in the expression for k. However, we shall treat this problem in detail for the sake of completeness. In going from Eq. (18a) to (18b) the large argument approximation for $K_0(jz(\xi))$ was used. If instead, an approximation corresponding to $k\rho' >> k\rho$ is used, one may then write

$$K_0(jk\sqrt{\rho^2+\rho'^2-2\rho\rho'\cos\xi}) \sim \frac{-j}{4}\sqrt{\frac{2}{\pi k\rho'}}\, e^{-j\left(k\rho' - \frac{\pi}{4}\right)} \left[2\pi e^{jk\rho\cos\xi}\right],$$

as given in Reference 4. Thus (18a) becomes

(38)

$$G(\bar{\rho},\bar{\rho}';\beta^{\mp}) \approx \frac{1}{4\pi^2 n}\left[\frac{-j}{4}\sqrt{\frac{2j}{\pi k\rho'}}\, e^{-jk\rho'}\right] \int_{L-L'} \frac{\pi}{j}\cot\left(\frac{\xi+\beta^{\mp}}{2n}\right) e^{jk\rho\cos\xi} d\xi.$$

If one suppresses the "line source factor " appearing in brackets, outside the integral of (38), then the resulting expression which may be denoted by $g^p(\rho,\beta^{\mp})$ is used to obtain total field, $g^p_{\substack{s\\h}}(\rho,\phi;\phi')$ due to a plane wave normally incident on the edge of the wedge. $g^p_{\substack{s\\h}}$ is given by

$$(39) \qquad g_{\substack{s\\h}}^{p}(\rho,\phi;\phi') = g^{p}(\rho,\beta^{-}) \mp g^{p}(\rho,\beta^{+}),$$

where for a plane wave of unit amplitude and zero phase at the edge,

$$(40) \qquad g^{p}(\rho,\beta^{\mp}) \equiv \frac{1}{4\pi jn} \int_{L-L'} \cot\left(\frac{\xi+\beta^{\mp}}{2n}\right) e^{jk\rho\cos\xi}\, d\xi \,.$$

Moreover, $g_{\substack{s\\h}}^{p}$ satisfies the 2-D, homogeneous scalar Helmholtz equation,

$$(41) \qquad (\nabla_t^2 + k^2)\, g_{\substack{s\\h}}^{p}(\rho,\phi;\phi') = 0,$$

the Dirichlet (s) and Neumann (h) boundary conditions on the surface of the wedge, and the Meixner edge condition. Thus, for an electric plane wave field $\hat{z}E^i$ incident on the wedge, the total electric field is given by

$$(42a) \qquad \bar{E} = \hat{z}\, E^i\, g_s^p \quad ,$$

whereas for a magnetic plane wave field $\hat{z}H^i$ incident on the wedge, the total magnetic field is

$$(42b) \qquad \bar{H} = \hat{z}\, H^i\, g_h^p.$$

The integral appearing in (40) has been extensively treated in Reference 14 where the generalized Pauli plane wave wedge diffraction coefficient was obtained via the method outlined in Appendix I. One might note that the integral over L-L' is evaluated exactly as done earlier for the canonical problem, where the SDP($\pm\pi$) closes the L-L' contours thereby facilitating the use of the Cauchy Residue

Theorem. Only the results for the diffracted fields (SDP($\pm\pi$) contributions) will be listed here, the geometrical optics terms being evaluated via the Residues of the integrand. Thus, the diffracted field $g_{\substack{s\\h}}^{p\,d}$ is given in terms of the scalar plane wave diffraction coefficient, $D_{\substack{s\\h}}$ as

$$(43) \qquad g_{\substack{s\\h}}^{p\,d} \sim D_{\substack{s\\h}} \frac{e^{-jk\rho}}{\sqrt{\rho}}$$

and is obtained for a largness parameter $\kappa = k\rho$.

$$(44) \qquad D_{\substack{s\\h}} = \{d^{+}(\beta^{-},n)\ F[\kappa a^{+}(\beta^{-})] + d^{-}(\beta^{-},n)\ F[\kappa a^{-}(\beta^{-})]\} \mp$$
$$\mp \{d^{+}(\beta^{+},n)\ F[\kappa a^{+}(\beta^{+})] + d^{-}(\beta^{+},n)\ F[\kappa a^{-}(\beta^{+})]\} ,$$

where

$$d^{\pm}(\beta,n) = -\frac{e^{-j\frac{\pi}{4}}}{n\sqrt{2\pi k}} \quad \frac{1}{2} \cot\left(\frac{\pi \pm \beta}{2n}\right) , \quad \beta = \beta^{\mp} \equiv \phi \mp \phi' .$$

Also,

$$(45) \qquad F[\kappa a^{\pm}(\beta)] = 2j\left|\sqrt{\kappa a^{\pm}(\beta)}\right| e^{j\kappa a^{\pm}(\beta)} \int_{\left|\sqrt{\kappa a^{\pm}(\beta)}\right|}^{\infty} e^{-j\tau^{2}} d\tau ,$$

where $\kappa = \kappa\rho$, and

$$(46) \qquad a^{\pm}(\beta) = \{1 + \cos(-\beta + 2nN^{\pm}\pi)\} .$$

The transition region correction factor $F[\kappa a^{\pm}(\beta)]$ tends to unity for $\kappa a^{\pm}(\beta) > 10$. When $F \to 1$ in all of the four terms in (44), $D_{\substack{s\\h}}$ reduces to the form given earlier in (27).

One obtains (44) by utilizing the results of Appendix I for evaluating

$$\int_{L-L'} F_1(\xi,\beta^{\mp})\, e^{\kappa f(\xi)}\, d\xi$$

via the modified steepest descent method, where $F(\xi,\beta^{\mp})$ and $f(\xi)$ are taken to be

$$F_1(\xi,\beta^{\mp}) = \frac{1}{4\pi jn} \cot\left(\frac{\xi+\beta^{\mp}}{2n}\right),$$

and

$$f(\xi) = j\cos\xi, \text{ with } \kappa = k\rho.$$

It can be shown that the complex ξ-plane topology is the same as in Fig. 4 with L-L' and SDP($\pm\pi$) contours unchanged. The integrand of (40) however has no branch point singularities.

C. Spherical Wave Illumination

Up to this point, only 2-D geometries have been treated. Consider now the case of a scalar point source illumination of the wedge. Let the point source be placed at $s'(\rho',\phi',z')$. The point source generates scalar, spherical waves. For a source of unit strength, the total field due to spherical waves incident on the impenetrable wedge is denoted by $g_{s_h}(\rho,\phi,z;\rho',\phi',z')$, where g_{s_h} satisfies

$$(47)\quad (\nabla^2+k^2)g_{s_h}(\bar{s},\bar{s}') = -\frac{\delta(\rho-\rho')\delta(\phi-\phi')\delta(z-z')}{\rho} = -\delta(|\bar{s}-\bar{s}'|).$$

$g_{s_h}(\bar{s},\bar{s}')$ is the scalar point source Green's function for the wedge, relating the field at $\bar{s}(\rho,\phi,z)$ due to a unit strength point source at $\bar{s}'(\rho',\phi',z')$.

$g_{s_h}(\bar{s},\bar{s}')$ satisfies the Sommerfeld radiation condition, the Meixner edge condition and the boundary conditions:

$$g_{s_h}(\bar{s},\bar{s}')\Big|_{\phi=0,n\pi} = 0, \quad \text{and} \quad \frac{\partial g_h(\bar{s},\bar{s}')}{\partial\phi}\Big|_{\phi=0,n\pi} = 0.$$

Note that $\nabla^2 = \nabla_t^2 + \frac{\partial^2}{\partial z^2}$ is the 3-D Laplacian operator. This 3-D problem may be reduced to a 2-D problem through a Fourier integral transformation. The z-variation may be removed via a Fourier transform on the z variable.

Thus,

$$(48) \qquad \tilde{g}_{s_h}(\rho,\phi,h;\rho',\phi',z') = \int_{-\infty}^{\infty} g_{s_h}(\bar{s},\bar{s}')e^{-jhz}\,dz$$

and by the uniqueness of the inverse transformation,

$$(49) \qquad g_{s_h}(\bar{s},\bar{s}') = \frac{1}{2\pi}\int_{-\infty}^{\infty} \tilde{g}_{s_h}(\rho,\phi,h;\rho',\phi',z')e^{jhz}\,dh.$$

The existence of the transform pair is assumed. Thus, Fourier transforming (47) yields

$$(50) \qquad (\nabla_t^2 + k_t^2)\tilde{g}_{s_h}(\rho,\phi,h;\rho',\phi',z') = \frac{-\delta(\rho-\rho')\delta(\phi-\phi')}{\rho}\,e^{-jhz'},$$

where

$$k_t^2 = k^2 - h^2.$$

Rewriting the above result as

$$(51) \qquad (\nabla_t^2 + k_t^2)\tilde{g}_{s_h}(\rho,\phi,h;\bar{s}')e^{jhz'} = -\delta(|\bar{\rho}-\bar{\rho}'|),$$

allows one to interpret $\tilde{g}_{\substack{s\\h}}(\rho,\phi,h;\bar{s}')e^{jhz'}$ as being identical to $G_{\substack{s\\h}}(\bar{\rho},\bar{\rho}')$ (2-D scalar line source Green's function of Eq. (4)) with the exception that k must now be replaced by k_t in Eq. (4). Thus, $\tilde{g}_{\substack{s\\h}} e^{jhz'}$ may be replaced by $G_{\substack{s\\h}}(\bar{\rho},\bar{\rho}';k_t)$.

The integral representation for $G_{\substack{s\\h}}(\bar{\rho},\bar{\rho}',k_t)$ is known, as it is equal to $G_{\substack{s\\h}}(\bar{\rho},\bar{\rho}';k)$ with k replaced by k_t, and is given by

$$G_{\substack{s\\h}}(\bar{\rho},\bar{\rho}';k_t) = G(\rho,\rho';\beta^-;k_t) \mp G(\rho,\rho';\beta^+;k_t) \tag{52}$$

or

$$\tilde{g}_{\substack{s\\h}}e^{jhz'} = \tilde{g}(\beta^-)e^{jhz'} \mp \tilde{g}(\beta^+)e^{jhz'}$$

where

(53)

$$\tilde{g}(\beta^{\mp})e^{jhz'} = G(\rho,\rho';\beta^{\mp};k_t) = \frac{1}{4\pi^2 n}\int_{L-L'}\frac{1}{2j}\cot\left(\frac{\xi+\beta^{\mp}}{2n}\right) K_o(jz(\xi))d\xi ,$$

as given by (18a), with $z(\xi)$ being

$$z(\xi) = k_t\sqrt{\rho^2+\rho'^2 - 2\rho\rho'\cos\xi} = \sqrt{k^2-h^2}\quad\sqrt{\rho^2+\rho'^2-2\rho\rho'\cos\xi}. \tag{54}$$

From the inverse Fourier transform relation,

$$g_{\substack{s\\h}}(\bar{s},\bar{s}') = g(\rho,z;\rho',z';\beta^-) \mp g(\rho,z;\rho',z';\beta^+) , \tag{55}$$

where

$$g(\rho,z;\rho',z';\beta) = \frac{1}{2\pi}\int_{\infty}^{\infty}\left[\int_{L-L'}\frac{1}{8\pi^2 jn}\cot\left(\frac{\xi+\beta}{2n}\right)K_o(jz(\xi))e^{-jh(z'-z)}d\xi\right]dh,$$

or

(56)

$$g(\rho,z;\rho',z';\beta) = \frac{-1}{32\pi^2 n} \int_{L-L'} d\xi \cot\left(\frac{\xi+\beta}{2n}\right) \cdot \int_{-\infty}^{\infty} dh\, H_0^{(2)}(\sqrt{k^2-h^2}\,\{\rho^2+\rho'^2-2\rho\rho'\cos\xi\}^{\frac{1}{2}}) e^{-jh(z'-z)},$$

where

$$K_\nu(jz) = -j\frac{\pi}{2} e^{-j\frac{\nu\pi}{2}} H_\nu^{(2)}(z)$$

has been used to obtain (56) from the preceeding equation. Further, it is known[19] that

$$\int_{\infty}^{\infty} dh\, H_0^{(2)}(\sqrt{k^2-h^2}\{\rho^2+\rho'^2-2\rho\rho'\cos\xi\}^{\frac{1}{2}})\, e^{-jh(z'-z)} \equiv 2j \frac{e^{-jk\sqrt{\rho^2+\rho'^2-2\rho\rho'\cos\xi+(z-z')^2}}}{\sqrt{\rho^2+\rho'^2-2\rho\rho'\cos\xi+(z-z')^2}}.$$

Utilizing the above result in (56) yields:

(57)

$$g(\rho,z;\rho',z';\beta) = \frac{-1}{16\pi^2 jn} \int_{L-L'} d\xi \cot\left(\frac{\xi+\beta}{2n}\right) \frac{e^{-jk\sqrt{\rho^2+\rho'^2-2\rho\rho'\cos\xi+(z-z')^2}}}{\sqrt{\rho^2+\rho'^2-2\rho\rho'\cos\xi+(z-z')^2}}.$$

The usefulness of the above point source scalar problem in the treatment of the vector electromagnetic problem is seen if one considers the case of either an electric or magnetic dipole moment ($e^{+j\omega t}$ time dependence assumed) which is $\hat{z}$ directed, and radiates in the presence of a wedge. The magnetic vector potential,

$\bar{A}$ at $\bar{s}$ (observation point) for an electric dipole moment of strength, $\hat{z}p_e\delta(|\bar{s}-\bar{s}'|)$ located at $\bar{s}'$, is given by

(58) $$\bar{A}(\bar{s}) = \hat{z}\mu p_e\, g_s(\bar{s},\bar{s}')$$

whereas the electric vector potential, $\bar{F}$ at $\bar{s}$ for a magnetic dipole moment of strength, $\hat{z}p_m\delta(|\bar{s}-\bar{s}'|)$, is given by

(59) $$\bar{F}(\bar{s}) = \hat{z}\varepsilon p_m\, g_h(\bar{s},\bar{s}').$$

Also,

(60) $$\bar{H}_e = \frac{\nabla\times\bar{A}}{\mu} \text{ and } \bar{E}_m = -\frac{\nabla\times\bar{F}}{\varepsilon},$$

where the subscripts e and m are used to denote field quan ties resulting from an electric dipole moment or a magnetic dipole moment, respectively. Thus, $\bar{H}_e$ = magnetic field intensity due to $\hat{z}p_e\delta(|\bar{s}-\bar{s}'|)$, whereas $\bar{E}_m$ = electric field intensity due to $\hat{z}p_m\delta(|\bar{s}-\bar{s}'|)$. An arbitrarily-polarized spherical wave can be generated by a superposition of the fields of these two dipoles.

Figure 5 depicts the geometry involving a point source at $\bar{s}'$ and the observation point at $\bar{s}$, for the source radiating in the presence of the wedge which is impenetrable. A coordinate transformation is now introduced. One is referred to Fig. 5 for details.

Let $\rho' = s' \sin\beta_0$ and $\rho = s \sin\beta_0$. Hence, $|(z-z')| = (s'+s)\cos\beta_0$, and

(61)

$$\rho^2+\rho'^2-2\rho\rho'\cos\xi + (z-z')^2 = (s'+s)^2\sin^2\beta_0 - 2s's\sin^2\beta_0(1+\cos\xi)+(s'+s)^2\cos^2\beta_0$$

$$= (s'+s)^2\left[1 - \frac{2s's\sin^2\beta_0}{(s'+s)^2}(1+\cos\xi)\right].$$

Incorporating the above result in (57) yields

$$(62)\quad g(\rho,z;\rho',z';\beta) = \frac{-1}{16\pi^2 jn}\int_{L-L'} d\xi \cot\left(\frac{\xi+\beta}{2n}\right)\cdot \frac{e^{-jk(s'+s)\sqrt{1-\frac{2s's\sin^2\beta_0}{(s'+s)^2}(1+\cos\xi)}}}{\sqrt{(s'+s)^2-2s's\sin^2\beta_0(1+\cos\xi)}}$$

As before, the integral over $L-L'$ is evaluated asymptotically for large $k\frac{s's}{s'+s}\sin^2\beta_0$, and the SDP($\pm\pi$) again close the L-L' contours allowing the use of the Cauchy Residue Theorem. The location of the SDP through saddle points at $\xi_s = \pm\pi$ and the complex ξ plane topology is once again unchanged except that the branch points of the integrand are now given by

$$\xi_b = 2\ell\pi \pm j\cosh^{-1}\frac{s'^2+s^2+2s's\cos^2\beta_0}{2s's\sin^2\beta_0},\quad \ell = 0,\pm1,\pm2,\cdots$$

and one is referred to Fig. 4 for details.

The asymptotic evaluation of the integral as in (62) is performed via the modified steepest descent method outlined in Appendix I, with $F_1(\xi)$ and $f(\xi)$ now given by

$$F_1(\xi) = \frac{-1}{16\pi^2 jn}\cot\left(\frac{\xi+\beta}{2n}\right)\frac{e^{-jk(s'+s)}}{\sqrt{(s'+s)^2-2s's\sin^2\beta_0(1+\cos\xi)}},$$

and

$$f(\xi) = j\,[1+\cos\xi]$$

where the approximation

$$(63)\quad e^{-jk(s'+s)}\sqrt{1-\frac{2s's\sin^2\beta_0}{(s'+s)^2}(1+\cos\xi)}$$
$$\approx e^{-jk(s'+s)}\left\{1-\frac{s's\sin^2\beta_0}{(s'+s)^2}(1+\cos\xi)\right\}$$

has been used in (62) for reasons identical to those involved in the approximation of Eq. (19).

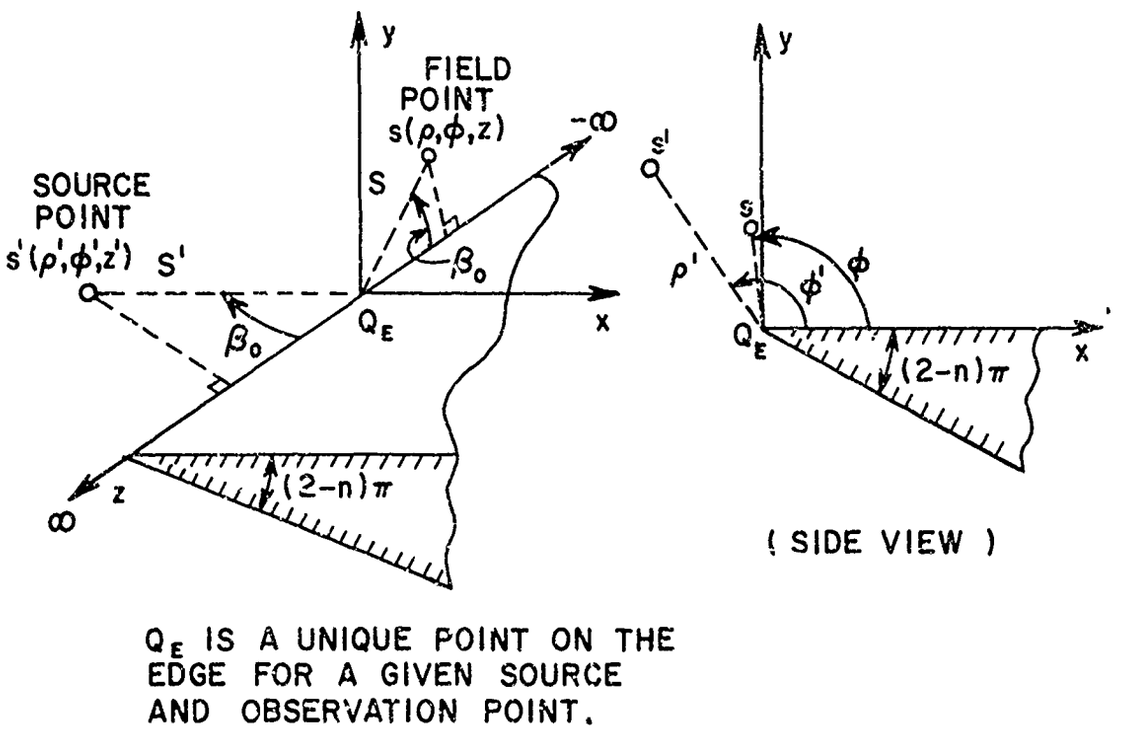

Fig. 4. Geometry for a point source illumination of the wedge.

The residues corresponding to the poles of $F_1(\xi)$ at $\xi = \xi_p = -\beta + 2nN\pi$ ($N=0, \pm1, \pm2, \cdots$), yield the geometrical optics fields (Note that $|\xi_p| \leq \pi$). The saddle point results yield the diffracted ray field component.

As before, the diffracted fields may be denoted by $g^d_{\substack{s \\ h}}(\bar{s},\bar{s}')$, where

$$(64)\quad g^d_{\substack{s \\ h}}(\bar{s},\bar{s}') = g^d(\rho,z;\rho',z';\beta^-) \mp g^d(\rho,z;\rho',z';\beta^+),$$

with

$$g^d(\rho,z;\rho',z';\beta^{\mp}) = -\int_{SDP(\pi)} F_1(\xi,\beta^{\mp})e^{\kappa f(\xi)} - \int_{SDP(-\pi)} F_1(\xi,\beta^{\mp})e^{\kappa f(\xi)}.$$

(Note that $\kappa = k\dfrac{s's}{s'+s}\sin^2\beta_o$ in this case).

No derivations are presented, but it can be shown by using the results of Appendix I, that

$$-\int_{SDP(\pm\pi)} F_1(\xi,\beta)e^{\kappa f(\xi)}d\xi \sim \pm \frac{e^{-jk(s'+s)}}{16\pi^2 jn(s'+s)}\sqrt{\frac{2\pi(s'+s)}{\kappa s's\sin^2\beta_o}}\, e^{j\left\{\begin{matrix}\frac{\pi}{4} \\ \frac{-3\pi}{4}\end{matrix}\right\}} \cdot$$

$$\cdot \cot\left(\frac{\pi\pm\beta}{2n}\right)\ F[\kappa a^{\pm}(\beta)],$$

which may be re-written as:

$$(65)\quad -\int_{SDP(\pm\pi)} F_1(\xi,\beta)e^{\kappa f(\xi)}d\xi \sim \pm\left[\frac{e^{-jks'}}{4\pi s'}\right]\left\{\frac{-e^{-j\pi/4}}{n\sqrt{2\pi k}}\ \frac{1}{2}\cot\left(\frac{\pi\pm\beta}{2n}\right)\right\}\frac{1}{\sin\beta_o}\cdot$$
$$\cdot\, F[\kappa a^{\pm}(\beta)]\sqrt{\frac{s'}{s\,(s'+s)}}\ e^{-jks}\ .$$

One is now able to interpret the asymptotic result in terms of the GTD, through a diffraction coefficient, $D_{\substack{s\\h}}$. Thus

$$(66)\quad g^d_{\substack{s\\h}} \sim \left[u^i = \frac{e^{-jks'}}{4\pi s'}\right]\ D_{\substack{s\\h}}\ \sqrt{\frac{s'}{s\,(s'+s)}}\ e^{-jks}$$

where

u^i = field of the unit source incident at the edge, and is given by

$u^i = \dfrac{e^{-jks'}}{4\pi s'}$, (and is equivalent to the point source, scalar Green's function in the absence of the wedge).

$$(67)\quad D_{\substack{s\\h}} = \left[\{d^+(\beta^-,n)F[\kappa a^+(\beta^-)] + d^-(\beta^-,n)F[\kappa a^-(\beta^-)]\}\ \mp\right.$$
$$\left.\mp\{d^+(\beta^+,n)F[\kappa a^+(\beta^+)] + d^-(\beta^+,n)F[\kappa a^-(\beta^+)]\}\right]\ \frac{1}{\sin\beta_o}\ ,$$

with

$$(68)\quad d^{\pm}(\beta,n) \equiv -\frac{e^{-j\pi/4}}{n\sqrt{2\pi k}}\ \frac{1}{2}\cot\ \frac{\pi\pm\beta}{2n}\ ,\ \beta=\beta^{\mp} \equiv \phi \mp \phi';$$

$$F[\kappa a^{\pm}(\beta)] = 2j\left|\sqrt{\kappa a^{\pm}(\beta)}\right|\ e^{jka^{\pm}(\beta)}\int_{\left|\sqrt{\kappa a^{\pm}(\beta)}\right|}^{\infty} e^{-j\tau^2}\,d\tau\ ,$$

in which

$$(69)\quad a^{\pm}(\beta) = \{1 + \cos(-\beta + 2nN^{\pm}\pi)\}, \qquad \kappa = \frac{ks's}{s'+s}\sin^2\beta_0,$$

and $N^{\pm}$ denotes the poles closest to each of the two saddle points. Once again, F may be looked upon as a transition region correction factor which tends to unity away from the transition boundaries or whenever $\kappa\, a^{\pm}(\beta) > 10$. The geometrical optics contribution may easily be shown to comprise of terms of the type

$$(70)\quad \frac{e^{-jk\sqrt{\rho^2+\rho'^2-2\rho\rho'\cos[-\beta+2nN^{\pm}\pi]}}}{4\pi\sqrt{\rho^2+\rho'^2-2\rho\rho'\cos[-\beta+2nN^{\pm}\pi]}}\; U[\pi-|-\beta+2nN^{\pm}\pi|\,].$$

If $F \to 1$ in (67), then D_{s_n} of (67) reduces to D_{s_h} as given in (27). The $(\sin\beta_0)^{-1}$ factor associated with D_{s_h} in (67) indicates a conical spreading of the rays in space as schematized in Fig. 5. This conical spreading of the diffracted rays is a consequence of Fermat's principle.

Summarizing the results derived thus far, one observes that the canonical problem of a line source wedge illumination (cylindrical wav. incidence) is useful in treating the subsequent scalar problems involving plane wave and spherical wave illuminations of the wedge. Separating the line source factor out from the integral formulation of the canonical problem yieldsthe solution for the plane wave incidence case, whereas a Fourier transformation related the spherical wave incidence case to the cylindrical wave incidence case.

The asymptotic approximation in each of the problems treated results in a solution which can be interpreted in terms of the geometrical theory of diffraction, and as expected, outside of the transition regions of the shadow and reflection boundaries, the diffraction coefficient is independent of the type of edge illumination. Within the transition regions, where strictly speaking, ray optics is no longer valid, the geometrical theory of diffraction can be used formally if one corrects the diffraction coefficients in the following simple manner. The scalar diffraction coefficients may be written as the sum of four terms, and each of these terms is multiplied by a function $F[\kappa a]$, see Eq. (32) for example.

$$|F(\kappa a)| \leq 1;$$

outside of the transition regions, where $\kappa a > 10$, $F[\kappa a] \approx 1$.

It is very interesting that $F[\kappa a]$ has precisely the same form for the different edge illuminations. The only difference for the different types of illumination occurs in it's argument; if we write $\kappa a = kLa$, then

$$L = \begin{cases} \rho & \text{for plane wave illumination} \\ \dfrac{\rho\rho'}{\rho + \rho'} & \text{for cylindrical wave illumination} \\ \dfrac{ss'}{s + s'} \sin^2\beta_0 & \text{for spherical wave illumination.} \end{cases}$$

To ensure the validity of the asymptotic solution, kL should be large.

It is indeed remarkable that the complex field behavior in the transition regions can be described in this compact, simple way.

In the next chapter we shall show how these scalar (acoustic) problems are related to the electromagnetic problem of a perfectly-conducting wedge illuminated by an arbitrarily polarized, plane, conical, cylindrical or spherical wave. It will be seen that the scalar diffraction coefficients developed in this chapter play an important role in the dyadic diffraction coefficient of the electromagnetic problem.

CHAPTER III
ELECTROMAGNETIC WEDGE DIFFRACTION

In Chapter II, the plane waves and the cylindrical waves associated with the uniform line source are normally incident on the edge of the wedge. The solutions of these scalar problems can be directly related to the corresponding electromagnetic problems, see (5) and (6) for the line source case and (42a,b) for the plane wave case. In this chapter the normally-incident waves of Chapter II will be generalized to obliquely-incident electromagnetic plane waves and obliquely-incident conical electromagnetic waves whose sources are traveling-wave line currents. In addition, the scalar spherical wave excitation will be generalized to an electromagnetic spherical wave. Arbitrarily-polarized, plane, conical and spherical waves may be treated by properly superimposing solutions of the electric and magnetic type. Asymptotic solutions to these more general problems and their interpretation in terms of the geometrical theory of diffraction form the material of this chapter.

However before taking up these problems, a ray-fixed coordinate system will be introduced. It will be seen that when this coordinate system is used, the resulting dyadic diffraction coefficient may be written compactly as the sum of two dyads, or alternatively, it may be written in matrix notation as a 2 x 2 diagonal matrix.

A. Coordinate Systems

The circular cylindrical coordinate system $(\rho,\phi,z;\rho',\phi',z')$ which we have used to treat wedge diffraction is an edge-fixed coordinate system. On the other hand, the rays incident and diffracted at Q_E in Fig. 4 are more conveniently described in terms of spherical coordinates centered at Q_E. Let the position of the source of the incident ray be defined by the coordinates (s',β_0',ϕ') and the point of diffraction, by the coordinates (s,β_0,ϕ) as shown in Fig. 5. The orthogonal unit vectors associated with these coordinates $(\hat{s}',\hat{\beta}_0',\hat{\phi}';\ \hat{s},\hat{\beta}_0,\hat{\phi})$ are ray fixed in contrast with the unit vectors $(\hat{\rho}',\hat{\phi}',\hat{z}';\hat{\rho},\hat{\phi},\hat{z})$.

The plane containing the incident ray and the edge of the wedge will be referred to as the plane of incidence, and the plane containing the diffracted ray and the edge of the wedge, as the plane of diffraction. The unit vector $\hat{I} = -\hat{s}'$ is in the direction of incidence and the unit vector $\hat{s}$ is in the direction of diffraction. It is apparent that the unit vectors $\hat{\beta}_0'$ and $\hat{\phi}'$ are parallel and perpendicular, respectively, to the plane of incidence, and the unit vectors $\hat{\beta}_0$ and $\hat{\phi}$ are parallel and perpendicular, respectively, to the plane of diffraction; moreover, $\hat{\beta}_0' = \hat{\phi}' \times \hat{I}$ and $\hat{\beta}_0 = \hat{\phi} \times \hat{s}$. It will be shown later that when the incident field is resolved into its parallel and perpendicular components and the diffracted field is resolved into its parallel and perpendicular components, the diffraction coefficient can be expressed as a 2 x 2 diagonal matrix, and in this sense the ray-

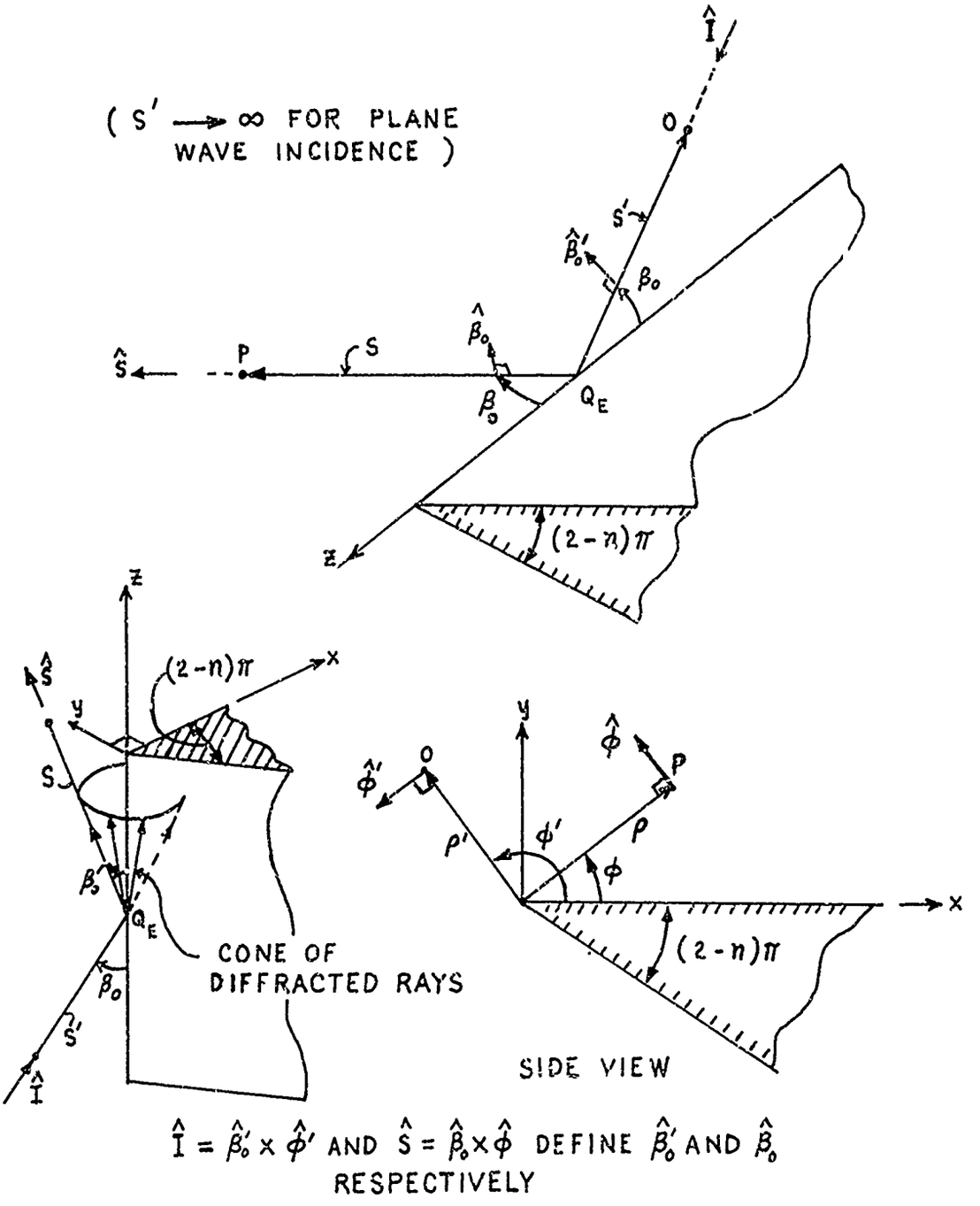

Fig. 5. Geometry for the ray coordinate system for electromagnetic wedge diffraction.

fixed coordinate system is a preferred coordinate system.

In the following sections the diffracted field components will first be determined in the edge-fixed coordinate system and then transformed to the ray-fixed coordinate system.

B. Plane Wave Illumination

The case of an arbitrarily-polarized, electromagnetic plane wave obliquely incident on a perfectly-conducting wedge is treated first. The geometry of the problem is depicted in Fig. 5. The incident electric field $\bar{E}^i$ may be decomposed into a component parallel to the plane of incidence $E_{\parallel}^i = \hat{\beta}_0' \cdot \bar{E}^i$, and a component perpendicular to the plane of incidence $E_{\perp}^i = \hat{\phi}' \cdot \bar{E}^i$. Thus, $\bar{E}^i = \hat{\beta}_0' E_{\parallel}^i + \hat{\phi}' E_{\perp}^i$, and $\bar{H}^i = \hat{\beta}_0' H_{\perp}^i + \hat{\phi}' H_{\parallel}^i$. The $\hat{z}$ components of $E_{\parallel}^i$ and $E_{\perp}^i$ are

$$(71) \qquad E_{\parallel z}^i = \hat{z} \cdot \bar{E}_{\parallel}^i = (\hat{\beta}_0' \cdot \bar{E}^i) \sin \beta_0 \quad \text{and} \quad E_{\perp z}^i = 0.$$

The $\hat{z}$ components of the magnetic fields associated with the parallel and perpendicular components of the incident electric field are

$$(72) \qquad H_{\parallel z}^i = 0 \text{ and } H_{\perp z}^i = \sqrt{\frac{\mu}{\varepsilon}} (\hat{\phi}' \cdot \bar{E}^i) \sin \beta_0.$$

(Note: $H_{\parallel}^i = \hat{\phi}' \cdot \bar{H}^i$ and $H_{\perp}^i = \hat{\beta}_0' \cdot \bar{H}^i$)

The total electric field intensity $\bar{E}$ and the total magnetic field intensity $\bar{H}$ in the region surrounding the wedge may be decomposed into total transverse (to $\hat{z}$) fields $(\bar{E}_t, \bar{H}_t)$ and total axial fields (E_z, H_z), respectively. Thus,

(73) $\quad \bar{E} = \bar{E}_t + \hat{z}\, E_z$ and $\bar{H} = \bar{H}_t + \hat{z}\, H_z$.

Let $G^o_{\substack{s\\h}}(\rho,\phi,z;\phi')$ represent the total field due to a "scalar" plane wave obliquely incident on an impenetrable wedge. $G^o_{\substack{s\\h}}(\rho,\phi,z;\phi')$ satisfies

$$(\nabla^2 + k^2)\, G^o_{\substack{s\\h}}(\rho,\phi,z;\phi') = 0.$$

A traveling wave dependence in z allows one to express $G^o_{\substack{s\\h}}(\bar{\rho};\phi')$ as

$$(74)\begin{cases} G^o_{\substack{s\\h}}(\bar{\rho};\phi') = g^p_{\substack{s\\h}}(\bar{\rho};\phi';k_t)\, e^{-jk_z z}, \text{ where} \\ k_z = k\cos\beta_o,\ (\nabla_t^2 + k_t^2)\, g^p_{\substack{s\\h}}(\rho,\phi;\phi;k_t) = 0, \\ \text{and } k_t = k\sin\beta_o. \end{cases}$$

$g^p_{\substack{s\\h}}(\rho,\phi;\phi',k_t)$ is identical to the expression for $g^p_{\substack{s\\h}}$ in (39) with k replaced by k_t.

It follows that

$$(75)\begin{cases} E_z = E^i_z\, g^p_s\, e^{-jk_z z} \\ \text{and} \\ H_z = H^i_z\, g^p_h\, e^{-jk_z z} \end{cases}$$

If one knows the solutions to the axial fields E_z and H_z, then one can evaluate $\bar{E}_t$ and $\bar{H}_t$ in terms of the axial fields from the results of Appendix II, given by the folowing relations

$$(76)\quad \bar{E}_t = -jk_z \frac{\nabla_t E_z}{k^2 - k_z^2} + j\omega\mu \frac{\hat{z} \times \nabla_t H_z}{k^2 - k_z^2},$$

$$\bar{H}_t = -jk_z \frac{\nabla_t H_z}{k^2 - k_z^2} - j\omega\varepsilon \frac{\hat{z} \times \nabla_t E_z}{k^2 - k_z^2}.$$

The above expressions are valid for problems which possess cylindrical uniformity in structure and fields.

The solutions for E_z and H_z are already known from Chapter II. The $\hat{z}$ components of the diffracted fields E_z^d and H_z^d, may be written in terms of the diffraction coefficient $D_{\substack{s \\ h}}$ of (44), but with k replaced by k_t. The total axial field is of course a superposition of the geometrical optics field and the diffracted ray field. Since this report is primarily concerned with the calculation of diffracted fields, only the results for the diffracted field will be presented here. It is a straight-forward matter to obtain the geometrical optics contributions via the residues at the poles associated with the incident and reflected fields, as was done in Chapter II, or, alternatively, the geometrical optics contributions can be deduced directly from physical considerations.

For the diffracted ray contribution to the axial fields, $g_{\substack{s \\ h}}^p(\rho,\phi;\phi';k_t)$ is replaced by $g_{\substack{s \\ h}}^{pd}$ as in (43) (but with k replaced by k_t). $g_{\substack{s \\ h}}^{pd}$ is in turn expressed in terms of $D_{\substack{s \\ h}}$ of (44), but with k replaced by k_t. Thus,

$$(77)\quad \begin{cases} E_z^d \sim E_z^i \sqrt{\sin\beta_o}\, D_s \dfrac{e^{-jk_t\rho}}{\sqrt{\rho}}\, e^{-jk_z z}, \\ \text{and} \\ H_z^d \sim H_z^i \sqrt{\sin\beta_o}\, D_h \dfrac{e^{-jk_t\rho}}{\sqrt{\rho}}\, e^{-jk_z z}, \end{cases}$$

where E_z^i, H_z^i are evaluated at Q_E, the point of incidence on the edge,

$$(78)\quad D_{\substack{s \\ h}} = \frac{1}{\sin\beta_o}\left[\{d^+(\beta^-,n)F[\kappa a^+(\beta^-)] + d^-(\beta^-,n)F[\kappa a^-(\beta^-)]\} \mp \right.$$
$$\left. \mp \{d^+(\beta^+,n)F[\kappa a^+(\beta^+)] + d^-(\beta^+,n)F[\kappa a^-(\beta^+)]\}\right],$$

with $\kappa = k_t\rho = k\rho \sin \beta_o$,

$$d^{\pm}(\beta,n) = \frac{-e^{-j\frac{\pi}{4}}}{n\sqrt{2\pi k}} \quad \frac{1}{2} \cot\left(\frac{\pi \pm \beta}{2n}\right) ,$$

$$F[\kappa a^{\pm}(\beta)] = 2j\left|\sqrt{\kappa a^{\pm}(\beta)}\right| e^{j\kappa a^{\pm}(\beta)} \int_{\left|\sqrt{\kappa a^{\pm}(\beta)}\right|}^{\infty} e^{-j\tau^2} d\tau ,$$

and $a^{\pm}(\beta) = 1 + \cos(-\beta + 2nN^{\pm}\pi)$, $\beta = \beta^{\pm} \equiv \phi \pm \phi'$. One may refer to Chapter II for the definition of $N^{\pm}$. From Fig. 5 it is evident that $\rho = s \sin \beta_o$. Also,

$$e^{-j(k_t\rho + k_z z)} = e^{-jks} \quad \text{(with } O_E \text{ as the origin).}$$

To evaluate $\bar{E}_t$ and $\bar{H}_t$, one may take the vector ∇_t and $\hat{z} \times \nabla_t$ operators within the integral

$$g^p(\rho,\phi;\phi';k_t) = \frac{1}{4\pi jn} \int_{L-L'} e^{jk_t\rho \cos \xi} \cot\left(\frac{\xi + \beta^{\mp}}{2n}\right) d\xi$$

where $g_{s,h}^p(\rho,\phi;\phi';k_t) = g^p(\rho,\phi;\phi';k_t) \mp g^p(\rho,\phi;\phi';k_t)$

(Note: as before, $g_s^p\Big|_{\phi=0,n\pi} = 0$, and $\frac{\partial g_h^p}{\partial \phi}\Big|_{\phi=0,n\pi} = 0$).

Thus,

$$(79) \quad \begin{cases} \nabla_t E_z \approx \hat{\rho} \dfrac{E_z^i e^{-jk_z z}}{4\pi jn} \left\{ \displaystyle\int_{L-L'} jk_t \cos \xi \, e^{jk_t\rho \cos \xi} \cdot \left[\cot\left(\frac{\xi + \beta^-}{2n}\right) - \cot\left(\frac{\xi + \beta^+}{2n}\right)\right] d\xi \right\}, \\ \nabla_t H_z \approx \hat{\rho} \dfrac{H_z^i e^{-jk_z z}}{4\pi jn} \left\{ \displaystyle\int_{L-L'} jk_t \cos \xi \, e^{jk_t\rho \cos \xi} \cdot \left[\cot\left(\frac{\xi + \beta^-}{2n}\right) + \cot\left(\frac{\xi + \beta^+}{2n}\right)\right] d\xi \right\}, \end{cases}$$

where E_z^i and H_z^i are, respectively, $E_{\parallel}^i \sin\beta_0$ and $H_{\perp}^i \sin\beta_0$ taken at Q_E.

The approximation involved in (79) is such that only those terms are retained, which on asymptotic evaluation yield terms of $O\left(\frac{1}{\sqrt{\rho}}\right)$. Higher order range dependent terms are neglected; this is a valid approximation if $k\rho$ is sufficiently large. The diffracted field contribution to $\nabla_t E_z$ and $\nabla_t H_z$ (denoted by $\nabla_t E_z^d$ and $\nabla_t H_z^d$ respectively) is obtained from the asymptotic approximation of (79) via the modified method of steepest descent described in Appendix I; one finds that

$$(80) \qquad \begin{Bmatrix} \nabla_t E_z^d \\ \nabla_t H_z^d \end{Bmatrix} \sim \hat{\rho} \begin{Bmatrix} E_z^i \\ H_z^i \end{Bmatrix} (-jk \sin^{3/2}\beta_0)\, D_{\substack{s \\ h}} \frac{e^{-jk_t\rho}}{\sqrt{\rho}}\, e^{-jk_z z}$$

with $D_{\substack{s \\ h}}$ in the above equation being identical to that of $D_{\substack{s \\ h}}$ in (78).

One may re-write (77) and (80) in terms of the parallel and perpendicular components of the incident field as

$$(81) \qquad \begin{Bmatrix} E_z^d \\ H_z^d \end{Bmatrix} \sim \begin{Bmatrix} E_{\parallel}^i \\ H_{\perp}^i \end{Bmatrix} \sin\beta_0\, D_{\substack{s \\ h}} \frac{e^{-jks}}{\sqrt{s}}$$

$$(82) \qquad \begin{Bmatrix} \nabla_t E_z^d \\ \nabla_t H_z^d \end{Bmatrix} \sim \hat{\rho} \begin{Bmatrix} E_{\parallel}^i \\ H_{\perp}^i \end{Bmatrix} (-jk \sin^2\beta_0)\, D_{\substack{s \\ h}} \frac{e^{-jks}}{\sqrt{s}}$$

Utilizing the above equations in (76), noting that $\hat{\rho} = \hat{s} \sin\beta_0 + \hat{\beta}_0 \cos\beta_0$, $\hat{z} = \hat{s} \cos\beta_0 - \hat{\beta}_0 \sin\beta_0$ and $\hat{z} \times \hat{\rho} = \hat{\phi}$, one obtains the following expressions for the diffracted fields $(\bar{E}^d, \bar{H}^d)$ expressed in terms of the coordinate system fixed in the diffracted ray

$$(83) \qquad \bar{E}^d = \bar{E}_t^d + \hat{z} E_z^d \sim -\hat{\beta}_0 E_{\parallel}^i D_s \frac{e^{-jks}}{\sqrt{s}} - \hat{\phi} E_{\perp}^i D_h \frac{e^{-jks}}{\sqrt{s}}$$

$$(84)\qquad \bar{H}^d = \bar{H}_t^d + \hat{z}H_z^d \sim -\hat{\beta}_o H_\perp^i D_h \frac{e^{-jks}}{\sqrt{s}} - \hat{\phi} H_\parallel^i D_s \frac{e^{-jks}}{\sqrt{s}}$$

The relations $H_\perp^i\sqrt{\mu/\varepsilon} = -E_\perp^i$ and $H_\parallel^i\sqrt{\mu/\varepsilon} = E_\parallel^i$ have been used to express the above results for $\bar{E}^d$ and $\bar{H}^d$ in terms of $(E_\parallel^i, E_\perp^i)$ and $(H_\perp^i, H_\parallel^i)$ respectively.

In equations (83) and (84) the incident-field is resolved into components parallel and perpendicular to the plane of incidence. Now if the diffracted field is expressed in terms of its components parallel and perpendicular to the plane of diffraction,

$$\bar{E}^d = E_\parallel^d\hat{\beta}_o + E_\perp^d\hat{\phi}\ ,$$

$$\bar{H}^d = H_\perp^d\hat{\beta}_o + H_\parallel^d\hat{\phi}\ ,$$

one may rewrite the above expressions in the form of the geometrical theory of diffraction.

$$\bar{E}^d \sim \bar{E}^i(Q_E)\cdot\bar{\bar{D}}_E\frac{e^{-jks}}{\sqrt{s}}$$

and

$$\bar{H}^d \sim \bar{H}^i(Q_E)\cdot\bar{\bar{D}}_H\frac{e^{-jks}}{\sqrt{s}}$$

where the dyadic diffraction coefficients $\bar{\bar{D}}_E(\phi,\phi';\beta_o)$ and $\bar{\bar{D}}_H(\phi,\phi';\beta_o)$ are expressed in the following simple form

$$(85)\qquad \begin{aligned}\bar{\bar{D}}_E(\phi,\phi',\beta_o) &= -\hat{\beta}_o'\hat{\beta}_o\, D_s(\phi,\phi',\beta_o) - \hat{\phi}'\hat{\phi}\, D_h(\phi,\phi',\beta_o)\\ \bar{\bar{D}}_H(\phi,\phi',\beta_o) &= -\hat{\beta}_o'\hat{\beta}_o\, D_h(\phi,\phi',\beta_o) - \hat{\phi}'\hat{\phi}\, D_s(\phi,\phi',\beta_o)\end{aligned}$$

where $D_{s,h}(\phi,\phi',\beta_0)$ is given by (78).

Expressing the diffraction coefficients in matrix notation

$$\begin{bmatrix} E_{\parallel}^{d} \\ E_{\perp}^{d} \end{bmatrix} \sim \begin{bmatrix} -D_s & 0 \\ 0 & -D_h \end{bmatrix} \begin{bmatrix} E_{\parallel}^{i}(Q_E) \\ E_{\perp}^{i}(Q_E) \end{bmatrix} \frac{e^{-jks}}{\sqrt{s}}$$

(86)

$$\begin{bmatrix} H_{\perp}^{d} \\ H_{\parallel}^{d} \end{bmatrix} \sim \begin{bmatrix} -D_h & 0 \\ 0 & -D_s \end{bmatrix} \begin{bmatrix} H_{\perp}^{i}(Q_E) \\ H_{\parallel}^{i}(Q_E) \end{bmatrix} \frac{e^{-jks}}{\sqrt{s}}$$

The diffraction coefficient reduces to a 2 x 2 diagonal matrix, because we have expressed the field components in the proper coordinate system, namely, the ray-fixed coordinate system, and because we retained only the range dependent terms of $O(1/\sqrt{\rho})$. Keller and Lewis have obtained the dyadic diffraction coefficient for a wedge in an edge-fixed coordinate system, where the incident and diffracted fields are expressed in terms of their cartesian components. They obtain a 3 x 3 matrix with 7 non-vanishing elements. Furthermore, unlike the results given here, their diffraction coefficient is not valid in the transition regions at the shadow and reflection boundaries. We have transformed our dyadic diffraction coefficient to the edge-fixed cartesian coordinate system. Outside of the transition regions, where the correction factors may be replaced by unity, our dyadic diffraction coefficient is identical with that of Keller and Lewis, which shows that the degree of approximation in the two asymptotic solutions is the same. Independently of our work, L.J. Kaplan* has shown that the Keller

*L.J. Kaplan, private communication.

and Lewis diffraction matrix can be reduced and diagonalized by a suitable matrix transformation.

C. Conical Wave Illumination

Consider next the diffraction of a conical electromagnetic wave by a perfectly-conducting wedge. At the edge the direction of incidence, which is normal to the conical wavefronts, is given by the unit vector $\hat{I}$; $\hat{I} \cdot \hat{z} = \cos \beta_0$, where $\pi/2 - \beta_0$ is the half-angle of the conical wavefronts. Conical waves may be generated by the electric and magnetic traveling-wave line currents $\hat{z}I\, e^{-jk_z z'}$ and $\hat{z}M\, e^{-jk_z z'}$, respectively, where I and M are complex constants and $k_z = k\cos \beta_0$.

The axial ($\hat{z}$-directed) incident electric field due to $Ie^{-jk_z z}$ and the axial incident magnetic field due to $Me^{-jk_z z}$ may be shown to be,

$$(87)\quad E_z^i = \frac{k_t^2}{j\omega\varepsilon} Ie^{-jk_z z'} \left[\frac{-j}{4} H_0^{(2)}(k_t\rho')\right], \text{ and}$$

$$H_z^i = \frac{k_t^2}{j\omega u} Me^{-jk_z z'} \left[\frac{-j}{4} H_0^{(2)}(k_t\rho')\right], \text{ respectively}$$

with $\quad k_t^2 \equiv k^2 - k_z^2 = k \sin \beta_0$.

The primes are used to denote a source-fixed coordinate system.

Next let us examine the conical wave behavior; the electric current line source will be treated. The fields of this source are

$$E_z^i = \frac{k_t^2}{j\omega\varepsilon} Ie^{-jk_z z'} \left[\frac{-j}{4} H_0^{(2)}(k_t\rho')\right], \quad H_z^i = 0$$

$$(88)\quad \bar{E}_t^i = -\hat{\rho}' \frac{jk_z}{k_t^2} \frac{\partial E_z}{\partial \rho'}, \text{ and } \bar{H}_t^i = -\hat{\phi}' \frac{j\omega\varepsilon}{k_t^2} \frac{\partial}{\partial \rho'} E_z.$$

For $k_t\rho'$ large, the Hankel function may be replaced by its asymptotic approximation, so that

$$\bar{E}^i = \left(\bar{E}_t^i + \hat{z}\, E_z^i\right) \sim I \frac{e^{-jk_z z'}}{j\omega\varepsilon} k_t \left[-\hat{\rho}' k_z + \hat{z}\, k_t\right] \left(\frac{-j}{4}\sqrt{\frac{2}{\pi k_t \rho'}}\; e^{-j\left(k_t\rho' - \frac{\pi}{4}\right)}\right),$$

(89)

$$\bar{H}^i = H_t^i \sim \hat{\phi}' I \left(\frac{-k_t}{4}\sqrt{\frac{2}{\pi k_t \rho'}}\; e^{-j\left(k_t\rho' - \frac{\pi}{4}\right)}\right) e^{-jk_z z'}.$$

$k_t\rho' + k_z z' = k(\rho' \sin\beta_0 + z' \cos\beta_0)$ = constant describes a conical surface and $\hat{I} \cdot \bar{E}^i$ and $\hat{I} \cdot \bar{H}^i$ both vanish; consequently, for $k_t\rho'$ large enough for the Hankel function of order zero to be replaced by it's asymptotic approximation, the electromagnetic field of a traveling-wave electric current line source is a conical wave with it's field vectors tangent to the wavefront, i.e., perpendicular to the associated rays. The electromagnetic field of the traveling-wave magnetic current line source has the same properties. In the case of the electric current line source, the incident electric field lies in the plane of incidence, whereas in the case of the magnetic current line source, it is perpendicular to the plane of incidence.

The total axial fields (E_z and H_z) excited by electric and magnetic traveling-wave line sources can be shown (see Appendix III) to be

(90)
$$\begin{cases} E_z = \dfrac{k_t^2}{j\omega\varepsilon}\, I e^{-jk_z z}\, G_s(\bar{\rho},\bar{\rho}';k_t), \text{ and} \\ H_z = \dfrac{k_t^2}{j\omega\mu}\, M e^{-jk_z z}\, G_h(\bar{\rho},\bar{\rho}';k_t), \text{ respectively.} \end{cases}$$

The special Green's function $G_{\substack{s\\h}}(\bar{\rho},\bar{\rho}';k_t)$ is the same as that of (4) with k replaced by k_t. As before,

$$(91)\qquad G_{\substack{s\\h}}(\bar{\rho},\bar{\rho}';k_t) = G(\rho,\rho';\beta^{-};k_t) \mp G(\rho,\beta';\ ^{+};k_t),$$

where the integral representation of $G(\rho,\rho';\beta^{\mp};k_t)$ is given by (18b) with k_t used in place of k. Also, the approximation of (19) is utilized in the exponent of the integrand in (18b). Specifically,

$$(92)\quad G(\rho,\rho';\beta^{\mp};k_t) \approx \frac{1}{8\pi^2 jn}\int_{L-L} \sqrt{\frac{\pi}{2jk_t(\rho^2+\rho'^2-2\rho\rho'\cos\xi)^{\frac{1}{2}}}}\cot\left(\frac{\xi+\beta^{\mp}}{2n}\right)\cdot e^{-jk_t(\rho+\rho')\left\{1-\frac{\rho\rho'}{(\rho+\rho')^2}(1+\cos\xi)\right\}}\,d\xi\ .$$

The diffracted ray contribution to (91) is known from the result of (28) in Chapter II from which the axial diffracted fields may be written as

$$(93)\begin{cases} E_z^d \sim \dfrac{k_t^2}{j\omega\varepsilon}\, Ie^{-jk_z z}\left(\dfrac{-j}{4}\sqrt{\dfrac{2}{\pi k_t\rho'}}\ e^{-j(k_t\rho'-\frac{\pi}{4})}\right) D_{\substack{s\\h}}\sqrt{\sin\beta_0}\ \dfrac{e^{-jk_t\rho}}{\sqrt{\rho}}\ , \\ \text{and} \\ H_z^d \sim \dfrac{k_t^2}{j\omega\mu}\, Me^{-jk_z z}\left(\dfrac{-j}{4}\sqrt{\dfrac{2}{\pi k_t\rho'}}\ e^{-j(k_t\rho'-\frac{\pi}{4})}\right) D_{\substack{h\\s}}\sqrt{\sin\beta_0}\ \dfrac{e^{-jk_t\rho}}{\sqrt{\rho}}\ , \end{cases}$$

where $D_{\substack{s\\h}}$ is identical to that of (78), but with κ equal to

$$\frac{k_t\rho\rho'}{\rho+\rho'} = \frac{k\rho\rho'}{\rho+\rho'}\sin\beta_0.$$

In terms of E_z^i and H_z^i which are the fields incident on the edge at Q_E, it is easily seen that (93) can be written as

$$(94)\qquad \begin{Bmatrix} E_z^d \\ H_z^d \end{Bmatrix} \sim \begin{Bmatrix} E_z^i \\ H_z^i \end{Bmatrix} \begin{matrix} D_s \\ h \end{matrix} \frac{e^{-jk_t\rho}}{\sqrt{\rho}}\, e^{-jk_z z} \sqrt{\sin\beta_o}$$

The transverse components of the diffracted fields may be obtained via (76) in the manner similar to that of the plane wave case treated earlier. The vector ∇_t and $\hat{z} \times \nabla_t$ operators are taken within the integral of (92) before carrying out the asymptotic evaluation.

$$(95)\begin{cases} \nabla_t E_z^d \sim -\hat{\rho} jk\, E_z^i\, D_s\, \sin^{3/2}\beta_o \dfrac{e^{-jk_t\rho}}{\sqrt{\rho}}\, e^{-jk_z z}, \\ \nabla_t H_z^d \sim -\hat{\rho} jk\, H_z^i\, D_h\, \sin^{3/2}\beta_o \dfrac{e^{-jk_t\rho}}{\sqrt{\rho}}\, e^{-jk_z z} \end{cases}$$

where $\begin{matrix} D_s \\ h \end{matrix}$ is identical to that of (78) but with $\kappa = \frac{k\rho\rho'}{\rho+\rho'} \sin\beta_o$.

In deriving (95), terms of $O(1/\sqrt{\rho})$ are retained; all higher order range dependent terms are negligible for $k_t\rho$ sufficiently large. One might observe that (94) and (77) possess identical forms as do (95) and (80), respectively.

Since $E_e^i = E_\parallel^i$ and $H_m^i = H_\perp^i$ in this problem, $E_z^i = E_e^i \sin\beta_o = E_\parallel^i \sin\beta_o$, and $H_z^i = H_\perp^i \sin\beta_o$. Also, $E_\perp^i = -\sqrt{\mu/\epsilon}\, H_\perp^i$, and $E_\parallel^i = \sqrt{\mu/\epsilon}\, H_\parallel^i$. Utilizing these results and the fact that $e^{-j(k_t\rho+k_z z)} = e^{-jks}$, (see Fig. 5), one may express (94) and (95) respectively as

$$(96)\qquad \begin{Bmatrix} E_z^d \\ H_z^d \end{Bmatrix} \sim \begin{Bmatrix} E_\parallel^i \\ H_\perp^i \end{Bmatrix} \begin{matrix} D_s \\ h \end{matrix} \sin\beta_o \frac{e^{-jks}}{\sqrt{s}}, \text{ and}$$

(Note: the subscripts e and m on E_e^i and H_m^i respectively denote the fields of electric and magnetic traveling-wave line sources.)

$$(97)\qquad \begin{Bmatrix} \nabla_t E_z^d \\ \\ \nabla_t H_z^d \end{Bmatrix} \sim \hat{\rho}\,(-jk) \begin{Bmatrix} E_{\parallel}^i \\ \\ H_{\perp}^i \end{Bmatrix} \underset{h}{D_s} \sin^2\beta_o \frac{e^{-jks}}{\sqrt{s}} \quad .$$

Equations (96) and (97) are similar in form to (81) and (82), respectively.

Following the procedure indicated for the vector plane wave incidence case, one may utilize (96) and (97) in (76) to obtain the total diffracted fields in the ray-fixed coordinate system. Then ($\bar{E}^d$ and $\bar{H}^d$) may be written in the form of the geometrical theory of diffraction as

$$(98)\begin{cases} \bar{E}^d \sim \bar{E}^i(Q_E) \cdot \underset{E}{\underset{H}{\bar{\bar{D}}}} \dfrac{e^{-jks}}{\sqrt{s}} \quad , \text{ and} \\ \bar{H}^d \sim \bar{H}^i(Q_E) \cdot \underset{E}{\underset{H}{\bar{\bar{D}}}} \dfrac{e^{-jks}}{\sqrt{s}} \quad . \end{cases}$$

Here, $\underset{E}{\underset{H}{\bar{\bar{D}}}}$ are the dyadic wedge diffraction coefficients for a conical wave excitation.

$$\underset{E}{\underset{H}{\bar{\bar{D}}}} = -\hat{\beta}_o'\hat{\beta}_o \underset{h}{D_s} - \hat{\phi}'\hat{\phi} \underset{s}{D_h} \ ,$$

and

$$\underset{h}{D_s} = \frac{1}{\sin\beta_o}\left[\{d^+(\beta^-,n)F[\kappa a^+(\beta^-)] + d^-(\beta^-,n)F[\kappa a^-(\beta^-)]\} \mp \right.$$

$$\left. \mp \{d^+(\beta^+,n)F[\kappa a^+(\beta^+)] + d^-(\beta^+,n(F[\kappa a^-(\beta^+)])\}\right] \quad ,$$

where the $d^{\pm}(\beta,n)$ terms are identical to the $d^{\pm}(\beta,n)$ given in (78) for the plane wave case. The form of $F[\kappa a^{\pm}(\beta)]$ is the same as in

(78) for the plane wave incidence case, except that κ in the correction factor $F[\kappa a]$ is equal to $\frac{k\rho\rho'}{\rho+\rho'} \sin\beta_0$ in this case. As the line source is removed from the edge $\rho' \to \infty$, the local illumination is plane wave and $\kappa \to k \sin\beta_0$, as it should.

When $\beta_0 = \pi/2$, which corresponds to uniform line source excitation (cylindrical wave incidence), then $D_{\substack{s\\h}}$ are given by (30). Finally, as the arguments of the transition region correction factors become large, i.e., when $\kappa a > 10$, the diffraction coefficients are equal to the $D_{\substack{s\\h}}$ given by (27) multiplied by $(\sin\beta_0)^{-1}$.

The matrix representation for (98) is given by (86).

D. Spherical Wave Illumination

The final vector wedge diffraction problem treated here is the diffraction of a spherical electromagnetic wave incident at Q_E along the direction $\hat{I}$ with an arbitrary field polarization transverse to $\hat{I}$. Such a spherical wave may be created by superimposing the fields of $\hat{z}$-directed electric and magnetic dipoles at s', see Fig. 5. The idea being that a general field may be constructed through a superposition of the TE (to $\hat{z}$) and TM (to $\hat{z}$) waves with the vector potentials $\bar{F}$ and $\bar{A}$, respectively[19]. The same principle was used in the previous problem of conical wave diffraction, where a superposition of electric and magnetic traveling-wave line source fields generated an arbitrarily-polarized conical wave.

As pointed out in Chapter II, Section C, $\bar{A}$ and $\bar{F}$ are given by $\bar{A}(\bar{s}) = \hat{z}\mu p_e g_s(\bar{s},\bar{s}')$ and $\bar{F}(\bar{s}) = \hat{z}\varepsilon p_m g_h(\bar{s},\bar{s}')$, respectively.

The electric dipole moment, $\hat{z}p_e\delta(|\bar{s}-\bar{s}'|)$ and the magnetic dipole moment, $\hat{z}p_m\delta(|\bar{s}-\bar{s}'|)$ generate the fields

$\bar{H}_e = \frac{1}{\mu} \nabla \times \bar{A}$ and $\bar{E}_m = -\frac{1}{\epsilon} \nabla \times \bar{F}$, respectively.

The Green's function $g_{\substack{s \\ h}}(\bar{s},\bar{s}')$ relates the field at $\bar{s}$ due to a source at $\bar{s}'$,

$$g_{\substack{s \\ h}}(\bar{s},\bar{s}') = g(\rho,z;\rho',z';\beta^-) \mp g(\rho,z;\rho',z';\beta^+),$$

where $g(\rho,z;\rho',z';\beta^{\mp})$ is given by (62). Now,

$$\bar{H}_e(\bar{s}) = \frac{1}{\mu} \nabla \times \hat{z}\mu p_e g_s(\bar{s},\bar{s}') = -\hat{z} \times \nabla_t p_e g_s(\bar{s},\bar{s}'),$$

and similarly

$$\bar{E}_m(\bar{s}) = \hat{z} \times \nabla_t p_m g_h(\bar{s},\bar{s}').$$

It can be verified quite easily that

$$(99)\quad -\hat{z} \times \nabla_t p_e g_s(\bar{s},\bar{s}') \approx \hat{\phi} \int_{L-L'} \frac{jkp_e(s'-s\cos\xi)}{16\pi^2 jn} \sin\beta_o \cot\left(\frac{\xi+\beta}{2n}\right) \cdot \frac{e^{k(s'+s)\left[-j+j\frac{s's\sin^2\beta_o}{(s'+s)^2}(1+\cos\xi)\right]}}{(s'+s)^2 - 2s's\sin^2\beta_o(1+\cos\xi)} d\xi,$$

where one retains only terms contributing a range dependence of $O(1/\rho)$. In deriving (99), it is convenient to use the Green's function in (57) rather than (62) so that the $\partial/\partial\rho$ and the $1/\rho\ \partial/\partial\phi$ operators of ∇_t can be applied directly. Following this operation, the transformation $\rho = s\sin\beta_o$ and $\rho' = s'\sin\beta_o$ may be used along with the approximation of (63); then, retaining the proper order of the range dependent terms, one obtains (99).

The complex ξ plane topology for $f(\xi) = j(1 + \cos \xi)$ is similar to that indicated in Fig. 3; however, the integrand of (99) has no branch cut singularities in the complex ξ plane. The diffracted rays corresponding to $\bar{H}_e$ may be obtained via the saddle point approximation of the integral of (99). Following the procedure outlined in Chapter II, the diffracted field, $\bar{H}_e^d$ may be expressed in terms of $I(\beta^{\mp})$, where

$$\hat{\phi} I(\beta^{\mp}) = -\hat{\phi} \int_{SDP(\pi)} \frac{jkp_e}{16\pi^2 jn} \frac{(s'-s\cos\xi)\sin\beta_0 e^{-jk(s+s')}}{(s'+s)^2-2ss'\sin^2\beta_0(1+\cos\xi)} \cot\left(\frac{\xi+\beta^{\mp}}{2n}\right) \cdot e^{\frac{jks's}{s'+s}\sin^2\beta_0(1+\cos\xi)} d\xi -$$

$$- \hat{\phi} \int_{SDP(-\pi)} \frac{jkp_e}{16\pi^2 jn} \frac{(s'-s\cos\xi)\sin\beta_0 e^{-jk(s+s')}}{(s'+s)^2-2ss'\sin^2\beta_0(1+\cos\xi)} \cot\left(\frac{\xi+\beta^{\mp}}{2n}\right) \cdot e^{\frac{jks's}{s'+s}\sin^2\beta_0(1+\cos\xi)} d\xi .$$

then

$$\bar{H}_e^d \sim \hat{\phi}[I(\beta^-) - I(\beta^+)] , \tag{100}$$

where

$$\beta^{\mp} \equiv \phi \mp \phi' .$$

$I(\beta^{\mp})$ is of course evaluated via the modified steepest descent method outlined in Appendix I. The geometrical optics component is again obtained from the residues at the poles of the integrand of (99). One may write $I(\beta^{\mp})$ as follows

$$(101)\quad \hat{\phi}I(\beta) \sim \hat{\phi}\left(jkp_e \frac{e^{-jks'}}{4\pi s'} \sin\beta_o\right) \frac{1}{4\pi jn} \frac{e^{j\frac{\pi}{4}}}{\sin\beta_o} \cot\left(\frac{\beta+\pi}{2n}\right)\sqrt{\frac{2\pi}{k}}\sqrt{\frac{s'}{s(s'+s)}}$$

$$\cdot e^{-jks}\, F[\kappa a^{+}(\beta)] \;-$$

$$-\hat{\phi}\left(jkp_e \frac{e^{-jks'}}{4\pi s'} \sin\beta_o\right) \frac{1}{4\pi jn} \frac{e^{-j\frac{3\pi}{4}}}{\sin\beta_o} \cot\left(\frac{\beta-\pi}{2n}\right)\sqrt{\frac{2\pi}{k}}\sqrt{\frac{s'}{s(s'+s)}}$$

$$\cdot e^{-jks}\, F[\kappa a^{-}(\beta)]\,,$$

where

$$F[\kappa a^{\pm}(\beta)] = 2j\left|\sqrt{\kappa a^{\pm}(\beta)}\right| e^{-j\kappa a^{\pm}(\beta)} \int_{\left|\sqrt{\kappa a^{\pm}(\beta)}\right|}^{\infty} e^{-j\tau^2}\, d\tau, \text{ and } \kappa = \frac{ks's}{s+s'} \sin^2\beta_o\,.$$

Rearranging terms in (101), and utilizing (100) allows one to write

$$(102)\quad \bar{H}_e^d \sim \hat{\phi}\,(jkp_e \frac{e^{-jks'}}{4\pi s'} \sin\beta_o) D_s \sqrt{\frac{s'}{s(s'+s)}}\; e^{-jks}$$

where D_s is given by (67).

In the ray optics approximation, one may use $\bar{E}_e^d = -\sqrt{\frac{\mu}{\varepsilon}}\,\hat{s} \times \bar{H}_e^d$ where $\hat{s}$ again denotes the direction of the diffracted ray. Using $\hat{s} \times \hat{\phi} = -\hat{\beta}_o$,

$$(103)\quad \bar{E}_e^d \sim \hat{\beta}_o (j\omega\mu p_e \frac{e^{-jks'}}{4\pi s'} \sin\beta_o)\, D_s \sqrt{\frac{s'}{s(s'+s)}}\, e^{-jks}\,.$$

One may recognize that the term $(j\omega\mu p_e \frac{e^{-jks'}}{4\pi s'} \sin\beta_o)$ represents the $-\hat{\beta}_o'$ component of the incident electric field radiated by the electric dipole moment evaluated at the point Q_E on the edge.

Again, $\bar{E}_e^i \cdot \hat{\beta}_o' = E_{\parallel}^i$ and thus,

$$(104)\quad \bar{E}_e^d \sim -\hat{\beta}_o\, E_{\parallel}^i\, D_s \sqrt{\frac{s'}{s(s'+s)}}\, e^{-jks}.$$

From duality, one may obtain $-\bar{E}_m^d$ via (100) on interchanging $\bar{H}_e^d$ by $-\bar{E}_m^d$, p_e by p_m, and D_s by D_h, respectively.

$$(105) \qquad -\bar{E}_m^d \sim \hat{\phi}(jkp_m \frac{e^{-jks'}}{4\pi s'} \sin\beta_o)\, D_h \sqrt{\frac{s'}{s(s'+s)}}\; e^{-jks},$$

where D_h is identical to that of (67). Alternatively, (105) may be obtained from $(\frac{1}{\varepsilon} \nabla \times \bar{F})$, where it is understood that only the diffracted field contribution of $(\frac{1}{\varepsilon} \nabla \times \bar{F})$ leads to (105).

Finally, $\bar{H}_m^d = (\hat{s} \times \bar{E}_m^d)\sqrt{\varepsilon/\mu}$ in the ray optics approximation, so that

$$(106) \qquad \bar{H}_m^d \sim \hat{\beta}_o\, (j\omega\varepsilon p_m \frac{e^{-jks'}}{4\pi s'} \sin\beta_o)\, D_h \sqrt{\frac{s'}{s(s'+s)}}\; e^{-jks}.$$

One may recognize $(jkp_m \frac{e^{-jks'}}{4\pi s'} \sin\beta_o)$ in (105) to be $E_\perp^i = \bar{E}_m^i \cdot \hat{\phi}'$. Similarly, $(j\omega\varepsilon p_m \frac{e^{-jks'}}{4\pi s'} \sin\beta_o)$ may be recognized to be $-H_\perp^i = -\bar{H}_m^i \cdot \hat{\beta}_o'$. Also $(jkp_e \frac{e^{-jks'}}{4\pi s'} \sin\beta_o)$ in (102) is equal to $-H_\parallel^i = -\bar{H}_e^i \cdot \hat{\phi}'$. Far-zone conditions for both the source and the field point are assumed in the above analysis; this is consistent with the desired ray-optical approximation. One may re-write (102), (104), (105) and (106) as

$$(107) \qquad \begin{cases} \bar{E}_e^d \sim -\hat{\beta}_o\, E_\parallel^i\, D_s \sqrt{\frac{s'}{s(s'+s)}}\; e^{-jks} \\ \bar{E}_m^d \sim -\hat{\phi}\; E_\perp^i\, D_h \sqrt{\frac{s'}{s(s'+s)}}\; e^{-jks} \\ \bar{H}_e^d \sim -\hat{\phi}\; H_\parallel^i\, D_s \sqrt{\frac{s'}{s(s'+s)}}\; e^{-jks} \\ \bar{H}_m^d \sim -\hat{\beta}_o\, H_\perp^i\, D_h \sqrt{\frac{s'}{s(s'+s)}}\; e^{-jks} \end{cases}$$

The total diffracted electric and magnetic field intensities are respectively

$$\bar{E}^d = \bar{E}^d_e + \bar{E}^d_m, \text{ and}$$

$$\bar{H}^d = \bar{H}^d_e + \bar{H}^d_m.$$

In terms of the dyadic diffraction coefficient $\bar{\bar{D}}_{\substack{E \\ H}}$

$$(108)\quad \begin{cases} \bar{E}^d \sim \bar{E}^i(Q_E) \cdot \bar{\bar{D}}_E \sqrt{\dfrac{s'}{s(s'+s)}}\ e^{-jks}, \text{ and} \\ \bar{H}^d \sim \bar{H}^i(Q_E) \cdot \bar{\bar{D}}_H \sqrt{\dfrac{s'}{s(s'+s)}}\ e^{-jks}, \text{ where} \end{cases}$$

$$\bar{\bar{D}}_{\substack{E \\ H}} = -\hat{\beta}'_o\hat{\beta}_o D_{\substack{s \\ h}} - \hat{\phi}'\hat{\phi}\, D_{\substack{h \\ s}}.$$

In the convenient matrix notation, (108) is given by

$$(109)\quad \begin{cases} \begin{bmatrix} E^d_{\parallel} \\ E^d_{\perp} \end{bmatrix} \sim \begin{bmatrix} -D_s & 0 \\ 0 & -D_h \end{bmatrix} \begin{bmatrix} E^i_{\parallel}(Q_E) \\ E^i_{\perp}(Q_E) \end{bmatrix} \sqrt{\dfrac{s'}{s(s+s')}}\ e^{-jks} \\ \begin{bmatrix} H^d_{\perp} \\ H^d_{\parallel} \end{bmatrix} \sim \begin{bmatrix} -D_h & 0 \\ 0 & -D_s \end{bmatrix} \begin{bmatrix} H^i_{\perp}(Q_E) \\ H^i_{\parallel}(Q_E) \end{bmatrix} \sqrt{\dfrac{s'}{s(s+s')}}\ e^{-jks} \end{cases}$$

As an example of the utility of the above results, let us consider the diffracted electric field of an arbitrarily-oriented electric dipole moment, $\hat{u}'\, p_e \delta(|\bar{s}-\bar{s}'|)$.

Let $\hat{u}'p_e = p_{e\rho'}\hat{\rho}' + p_{e\phi'}\hat{\phi}' + p_{ez'}\hat{z}'$, where $p_{e\rho'}$, $p_{e\phi'}$ and $p_{ez'}$ are the components of $\hat{u}'p_e$ in the $\hat{\rho}'$, $\hat{\phi}'$ and $\hat{z}'$ directions, respectively. Table I gives $E^i_{\parallel}$ and $E^i_{\perp}$ for these components.

TABLE I

electric dipole orientation	$E_{\parallel}^{i} = \hat{\beta}_0' \cdot \bar{E}^{i}$	$E_{\perp}^{i} = \hat{\phi}' \cdot \bar{E}^{i}$
$p_{e\rho}, \hat{\rho}'$	$-jkp_{e\rho}, \frac{e^{-jks'}}{4\pi s'} \cos \beta_0$	0
$p_{e\phi}, \hat{\phi}'$	0	$jkp_{e\phi}, \frac{e^{-jks'}}{4\pi s'}$
$p_{ez}, \hat{z}'$	$-jkp_{ez}, \frac{e^{-jks'}}{4\pi s'} \sin \beta_0$	0

The diffracted electric field is readily found by substituting $E_{\parallel}^{i}$, $E_{\perp}^{i}$ into (109).

The preceding results were derived for $0 < \phi' < n\pi$. If the analyses are repeated for $\phi' = 0, n\pi$, i.e., for grazing incidence along the surface of the wedge, in each case the diffraction coefficients D_h are multiplied by a factor of 1/2 and the diffraction coefficients $D_s = 0$. This also may be deduced by considering grazing incidence as the limit of oblique incidence. At grazing incidence, the incident and reflected fields merge, so that 1/2 of the total field propagating along the face of the wedge toward the edge is the incident field and the other 1/2 is the reflected field.

CHAPTER IV

DISCUSSION

It has been shown that when electromagnetic plane, cylindrical, conical and spherical waves are incident on a perfectly-conducting wedge the resulting diffraction can be approximated asymptotically in the form of the geometrical theory of diffraction. Summarizing the results of Chapters II and III, the diffracted electric field

$$\bar{E}^d(s) = \bar{E}^i(Q_E) \cdot \bar{\bar{D}}_E(\hat{s},\hat{I})A(s)e^{-jks} \tag{110}$$

where $\bar{E}^i(Q_E)$ is the incident electric field at the point of diffraction,

$A(s)$ is the spatial attenuation which describes how the field intensity varies along the diffracted ray,

$$A(s) = \begin{cases} \dfrac{1}{\sqrt{s}} & \text{for plane, cylindrical, and conical wave incidence (s is replaced by } \rho \text{ in the case of cylindrical wave incidence),} \\ \sqrt{\dfrac{s'}{s(s'+s)}} & \text{for spherical wave incidence,} \end{cases} \tag{111}$$

$\bar{\bar{D}}_E(\hat{s},\hat{I})$ is the dyadic diffraction coefficient,

$$\bar{\bar{D}}_E = -\hat{\beta}_0'\hat{\beta}_0 D_s(\phi,\phi';\beta_0) - \hat{\phi}'\hat{\phi} D_h(\phi,\phi';\beta_0), \tag{112}$$

$$(113)^{*}\quad D_{\substack{s\\h}} = \frac{1}{\sin\beta_0}\left[\{d^{+}(\beta^{-},n)F[\kappa a^{+}(\beta^{-})] \mp d^{-}(\beta^{-},n)F[\kappa a^{-}(\beta^{-})]\}\right.$$

$$\left.\mp\{d^{+}(\beta^{+},n)F[\kappa a^{+}(\beta^{+})] + d^{-}(\beta^{+},n)F[\kappa a^{-}(\beta^{+})]\}\right] \text{ , where}$$

$$(114)\quad d^{\pm}(\beta,n) = -\frac{e^{-j\frac{\pi}{4}}}{n\sqrt{2\pi k}}\ \frac{1}{2}\cot\frac{\pi\pm\beta}{2n}\ \text{, in which } \beta = \beta^{\mp} \equiv (\phi\mp\phi')$$

and

$$(115)\quad F[\kappa a^{\pm}(\beta)] = 2j\left|\sqrt{\kappa a^{\pm}(\beta)}\right| e^{j\kappa a^{\pm}(\beta)} \int_{\left|\sqrt{\kappa a^{\pm}(\beta)}\right|}^{\infty} e^{-j\tau^{2}}\, d\tau.$$

The parameters which appear in $F[\kappa a^{\pm}(\beta)]$ are defined below

$$(116)\qquad a^{\pm}(\beta) = 1 + \cos(-\beta + 2n\mathrm{N}^{\pm}\pi)$$

in which $N^{\pm}$ is the positive or negative integer or zero, which most nearly satisfies the equations

$$(117)\quad \begin{cases} 2n\pi N^{-} - \beta = -\pi\ , \\ 2n\pi N^{+} - \beta = \pi. \end{cases}$$

$\kappa = kL$ is the largeness parameter in the asymptotic evaluation of the pertinent integrals involved in the formulation of the dyadic diffraction coefficient. The quantity L (appearing in $\kappa = kL$) may be viewed as a distance parameter which depends upon the type of edge illumination; it is given by

$$(118)\quad L = \begin{cases} s\sin^{2}\beta_0 & \text{for plane waves,} \\ \dfrac{\rho'\rho}{\rho+\rho'} & \text{for cylindrical waves,} \\ \dfrac{s's\sin^{2}\beta_0}{s+s'} & \text{for conical and spherical waves.} \end{cases}$$

*For grazing incidence ($\phi'=0,n\pi$), see discussion at the end of Ch. III.

When the ray-fixed coordinate system is employed, the dyadic diffraction coefficient may be expressed as the sum of two dyads. One of the dyads involves D_s, the scalar diffraction coefficient for the Dirichlet boundary condition, and the other, D_h, the scalar diffraction coefficient for the Neumann boundary condition. In turn D_s, D_h depend upon trigonometric functions which appear in $d^{\pm}(\beta,n)$ and $F[\kappa a^{\pm}(\beta)]$, which involves a Fresnel integral. The latter may be regarded as a correction factor to be used in the transition regions of the shadow and reflection boundaries. Outside of the transition regions where, $\kappa a^{\pm}(\beta) = kLa^{\pm}(\beta) > 10$, F is approximately equal to one. Even within a transition region, usually only one of the four correction factors in (113) is significantly different from unity. Curves of the magnitude and phase of F as a function of kLa are presented in Fig. 6.

Two important approximations have been made in deriving (110). In accordance with the geometrical theory of diffraction, it has been assumed that the high-frequency diffracted field propagates along it's ray path in the same manner as the geometrical optics field. Consequently, the diffracted electric and magnetic fields in our asymptotic solution are perpendicular to their direction of propagation. This approximation does not introduce serious error if both the source point and the field point are far from the edge. Secondly, in deriving (110) it has been assumed that kL is large. However, based on the extensive numerical study of asymptotic solutions of this type presented in Reference 9, it would appear that generally

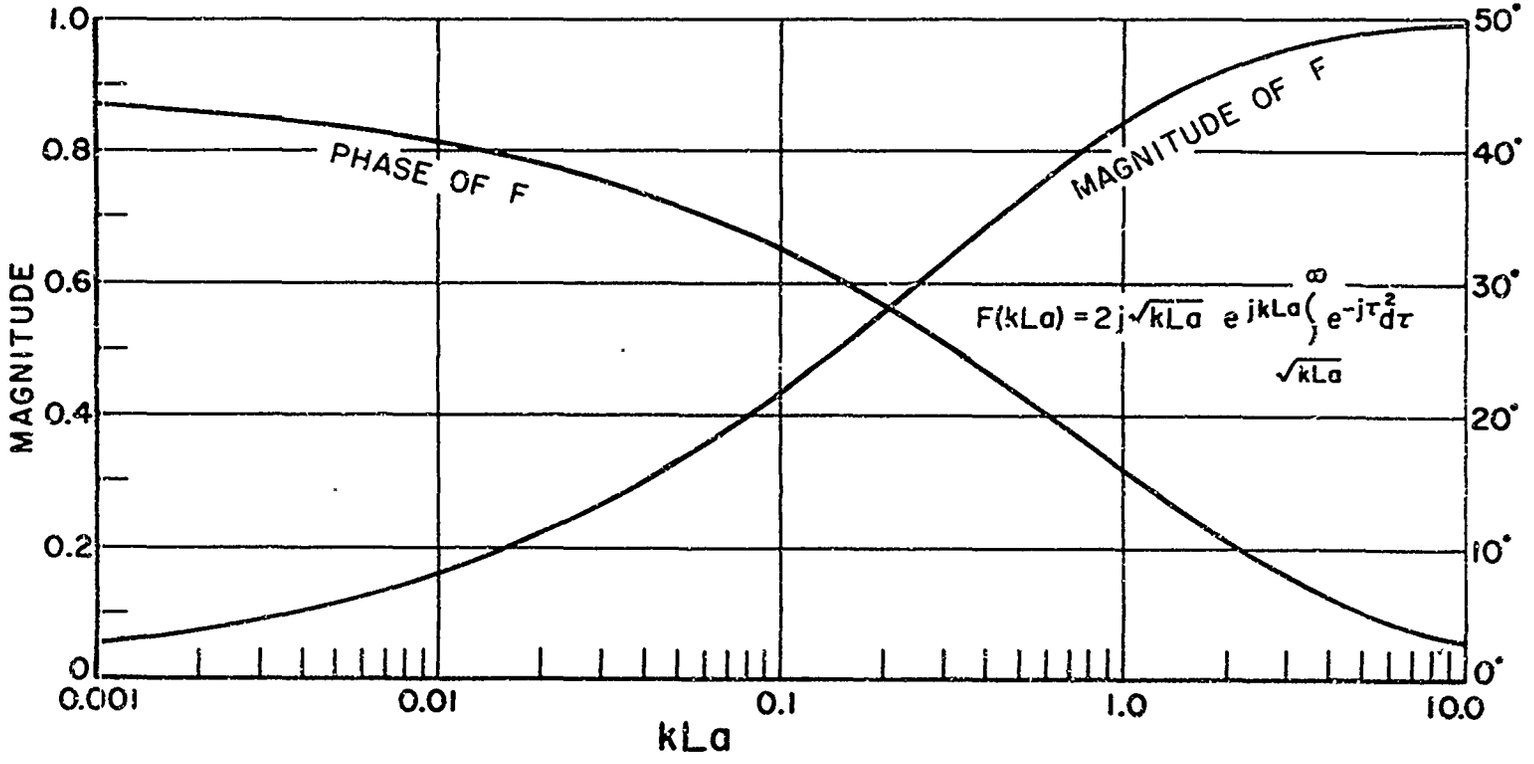

Fig. 6. Transition region correction factor F(kLa) (the positive branch of $\sqrt{kLa}$ is taken).

speaking this approximation introduces serious error only when $kL < 1$. It should be noted that the accuracy of (110) depends on both approximations, and a study of the error introduced by the two approximations, when either the source point or the field point (or both points) are close to the edge has not been carried out.

The preceding discussion has been restricted to the diffraction by wedges with straight edges; however the geometrical theory of diffraction may be used to treat the diffraction from curved edges.[1,2] The diffracted ray paths are determined by the generalized Fermat's principle for edge diffraction, and the conservation of power flow in the resulting astigmatic bundle of rays, see Fig. 7a, leads to the general spatial attenuation factor

$$A(s) = \sqrt{\frac{\rho_c}{s(\rho_c + s)}} \tag{119}$$

where the caustic distance ρ_c shown in Fig. 7a is given by

$$\frac{1}{\rho_c} = \frac{1}{s'} - \frac{\hat{n} \cdot (\hat{I} - \hat{s})}{\rho_e \sin^2 \beta_o} \tag{120}$$

for spherical wave illumination of the edge.[21] In the equation above

ρ_e is the radius of curvature of the edge,

$\hat{n}$ is the unit vector normal to the edge,

$\hat{I}, \hat{s}$ are unit vectors in the directions of incidence and diffraction, respectively.

β_o is the angle between $\hat{I}$ and $\hat{e}$, the tangent to the edge at the point of diffraction - see Fig. 7b.

The expression for A(s) given in (119) reduces to that given in (111), if ρ_e is set equal to infinity for the straight edge; furthermore,

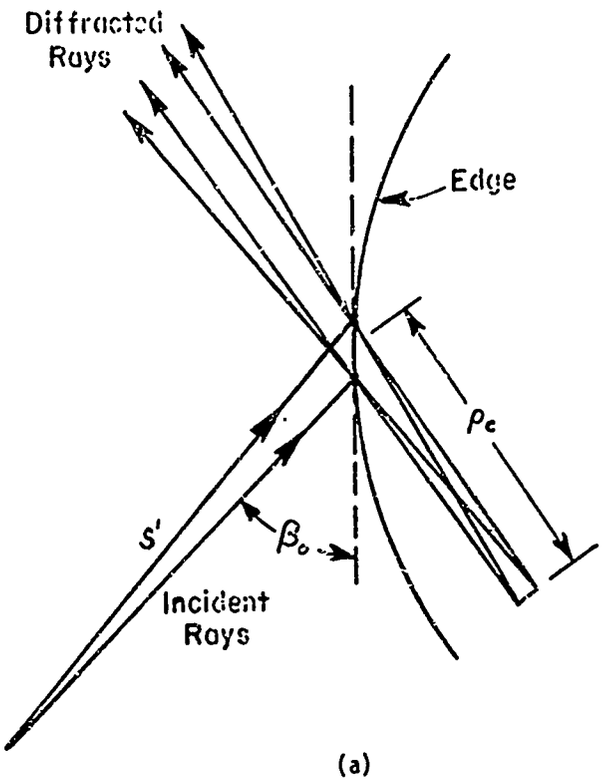

(a)

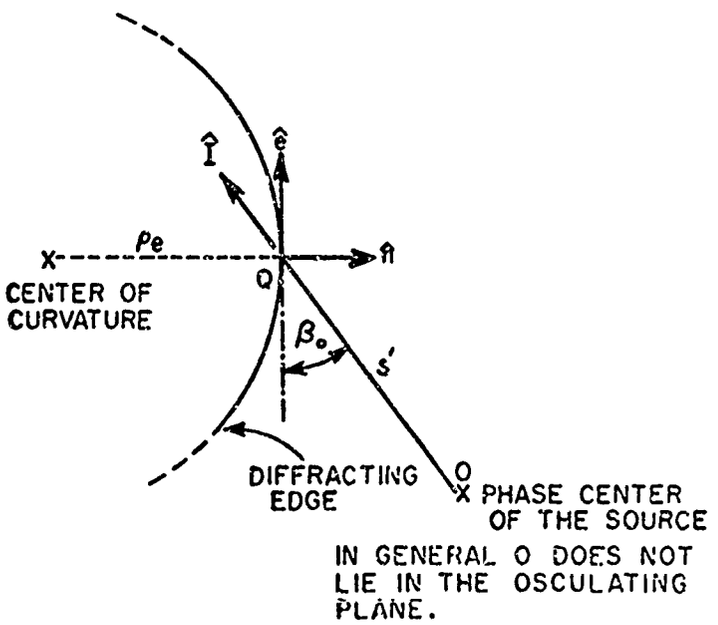

(b)

Fig. 7. Diffraction at a curved edge.

for plane, cylindrical and conical wave illumination of the straight edge, $\rho_c = \infty$.

The diffraction coefficient is assumed to be independent of ρ_e to a first approximation; this is a reasonable assumption because it is independent of the curvature of the incident wavefront to this approximation, as has been demonstrated here in Chapters II and III. Furthermore, the validity of this assumption has been confirmed in numerous applications of the geometrical theory of diffraction to structures with curved edges. Thus in accordance with the postulates of the geometrical theory of diffraction, (110) becomes

$$\bar{E}^d(\bar{s}) = \bar{E}^i(Q_E) \cdot \bar{\bar{D}}_E(\hat{s},\hat{i}) \sqrt{\frac{\rho_c}{s(\rho_c + s)}}\, e^{-jks}, \tag{121}$$

where $\bar{\bar{D}}_E$ is given by Eq. (112). Alternatively, if the incident and diffracted electric fields are resolved into components parallel and perpendicular to the planes of incidence and diffraction, respectively, one may write (121) in terms of matrix notation as

$$\begin{bmatrix} E_{\parallel}^d \\ E_{\perp}^d \end{bmatrix} = \begin{bmatrix} -D_s & 0 \\ 0 & -D_h \end{bmatrix} \begin{bmatrix} E_{\parallel}^i \\ E_{\perp}^i \end{bmatrix} \sqrt{\frac{\rho_c}{s(\rho_c + s)}}\, e^{-jks}. \tag{122}$$

By introducing the proper ray-fixed coordinate system the polarization effects of high-frequency scattering may be greatly simplified, whether this involves the reflection from a smooth curved surface, the diffraction from an edge, or the diffraction from a smooth curved surface. Specifically, the polarization of the scattered field may be related to the polarization of the incident field by a 2 x 2 diagonal matrix. In the case of reflection

one resolves the incident and reflected fields into components parallel and perpendicular to the plane of incidence, as is well known, and in the case of diffraction by a smooth curved surface, one resolves the incident and diffracted fields into components parallel and perpendicular to the planes of incidence and diffraction, respectively, where the plane of diffraction in this case contains the normal to the surface at the point of diffraction and the diffracted ray.[2]

In summary, employing the modified Pauli-Clemmow method of steepest descent and introducing a ray-fixed coordinate system, a compact, dyadic diffraction coefficient has been found for the perfectly-conducting wedge. This diffraction coefficient is valid in the transition regions of the shadow and reflection boundaries for a variety of edge illuminations. From a practical viewpoint, this diffraction coefficient is of value in applying the geometrical theory of diffraction to antenna and scattering problems involving three-dimensional structures with edges.

APPENDIX I
MODIFIED STEEPEST DESCENT METHOD
FOR A POLE SINGULARITY NEAR THE SADDLE POINT

Given

$$I(\kappa) = \int_C F_1(\xi)\, e^{\kappa f(\xi)}\, d\xi, \tag{A-1}$$

and the contour c is a path of integration in the complex ξ plane such that the integral converges. The following procedure outlines the approximate evaluation of $I(\kappa)$ for large κ, where κ is real.

Let $f(\xi)$ possess a saddle point at $\xi = \xi_s$ (i.e., $df/d\xi = 0$ at $\xi = \xi_s$), and further, let $F_1(\xi)$ possess a simple pole type singularity at $\xi = \xi_p$. The procedure to be outlined allows for ξ_p to lie in the vicinity of ξ_s.

The contour c is deformed so that it passes through ξ_s along the steepest descent path (SDP). If any singularities of the integrand are traversed in the deformation of c to the SDP, their contributions must be properly accounted for in the evaluation of the integral.

The SDP in the complex ξ plane is given by the equation

$$\text{Im } f(\xi) = \text{Im } f(\xi_s), \text{ (subject to Re } f(\xi) < 0 \text{ for } |\xi| \to \infty). \tag{A-2}$$

The SDP in the ξ plane may be mapped into a straight line along the Re μ axis in the complex μ plane via the transformation

$$f(\xi) = f(\xi_s) - \mu^2. \tag{A-3}$$

Further, the descending part of the SDP is mapped onto the positive μ axis (this determines the choice of the branch of μ in Eq. (A-3). Thus

$$I(\kappa) = e^{\kappa f(\xi_s)} \int_{-A}^{B} e^{-\kappa\mu^2} F_1(\xi) \frac{d\xi}{d\mu}\, d\mu, \quad -A \leq \mu \leq B.$$

Assuming that $\frac{d\xi}{d\mu}$ is analytic in the nbhd of ξ_s, let

$$F_2(\mu) = F_1(\xi) \frac{d\xi}{d\mu} [f(\xi) - f(\xi_p)] \quad . \tag{A-4}$$

$F_2(\mu)$ is now analytic in the nbhd of ξ_p and ξ_s. Thus,

$$F_2(\mu) = \sum_{m=0}^{\infty} c_m \mu^m, \tag{A-5}$$

and is a valid representation for $F_2(\mu)$ about the saddle point. Let

$$f(\xi) - f(\xi_p) = f(\xi_s) - f(\xi_p) - \mu^2 = -(\mu^2 + ja), \tag{A-6}$$

where

$$a \equiv j [f(\xi_s) - f(\xi_p)] \quad . \tag{A-7}$$

Using (A-4), (A-5), and (A-7) in $I(\kappa)$ yields

$$I(\kappa) = -e^{\kappa f(\xi_s)} \int_{-A}^{B} \frac{F_2(\mu) e^{-\kappa\mu^2}}{\mu^2 + ja} \, d\mu \approx -e^{\kappa f(\xi_s)} \cdot c_0 \int_{-A}^{B} \frac{e^{-\kappa\mu^2} \, d\mu}{\mu^2 + ja} \quad , \tag{A-8}$$

if one retains only the first term in the MacLauren expansion for $F_2(\mu)$. This leads to the first order saddle point result. In the asymptotic approximation one may extend the limits of integration from $-\infty$ to ∞, since the dominant contribution to the integral is from the immediate nbhd of the saddle point at $\mu = 0$ when κ is sufficiently large, and elsewhere the integrand falls off extremely rapidly, contributing negligibly to the integral. Therefore, (A-8) becomes:

$$I(\kappa) \sim -e^{\kappa f(\xi_s)} c_0 \int_{-\infty}^{\infty} \frac{e^{-\kappa\mu^2}}{\mu^2 + ja} \, d\mu \quad . \tag{A-9}$$

From the relation $f(\xi)-f(\xi_p) = -(\mu^2+ja)$ of (A-6) it follows that

$$\left.\frac{d\xi}{d\mu}\right|_{\mu=0} = \sqrt{\frac{-2}{f''(\xi_s)}} \ ,$$

so that

$$c_0 = F_2(\xi_s) = F_1(\xi_s)\left\{\sqrt{\frac{-2}{f''(\xi_s)}}\right\} \quad (-ja).$$

The choice of the proper sign on $\left.\frac{d\xi}{d\mu}\right|_{\mu=0}$ is determined by the direction of integration along the SDP in the ξ-plane. It can be shown that

$$\int_{-\infty}^{\infty} \frac{e^{-\kappa\mu^2}}{\mu^2 + ja}\, d\mu = 2e^{j\kappa a}\sqrt{\frac{\pi}{a}} \int_{\sqrt{\kappa a}}^{\infty} e^{-j\tau^2}\, d\tau.$$

Thus, it follows that (A-9) can be finally written as

$$\text{(A-10)} \qquad I(\kappa) \sim e^{\kappa f(\xi_s)} F_1(\xi_s) \left| \sqrt{\frac{-2\pi}{\kappa f''(\xi_s)}} \right| e^{j\phi_s} \quad F[\kappa a] \ ,$$

where ϕ_s accounts for the argument of $\sqrt{-2/f''(\xi_s)}$, and where

$$\text{(A-11)} \qquad F[\kappa a] = 2j\left|\sqrt{\kappa a}\right| e^{j\kappa a} \int_{\left|\sqrt{\kappa a}\right|}^{\infty} e^{-j\tau^2}\, d\tau \ ,$$

$F[\kappa a]$ may be viewed as a factor which accounts for the effect of the pole of $F_1(\xi)$ which may lie in the vicinity of the saddle point. When $\kappa a \to \infty$, $F[\kappa a] \to 1$, and for $\kappa a > 10$, $F[\kappa a] \approx 1$. Thus, when the pole singularity is sufficiently far removed from the saddle point, $F[\kappa a]$ may be replaced by unity, and (A-10) becomes

$$\text{(A-12)} \qquad I(\kappa) \sim e^{\kappa f(\xi_s)} F_1(\xi_s) \left| \sqrt{\frac{-2\pi}{\kappa f''(\xi_s)}} \right| e^{j\phi_s} \ ,$$

which is the well known first order asymptotic result for the case of pole not close to the saddle point. The techniques developed in this appendix may be referred to as the "Pauli-Clemmow modification of the method of steepest descent".

For those who are interested, the mapping of the ξ plane onto the μ plane is shown in Fig. 8. Although there are two isolated, first order saddle points in the ξ plane (see Fig. 3), it should be noted that only a single saddle point can occur in the μ plane. Thus only a finite region of the ξ plane, adjacent to a given SDP, is mapped onto the μ plane. In the present case there are two SDP's and thus there are two finite regions to be mapped in the ξ plane; one is defined by $(0 \leq u \leq 2\pi, -\infty < v < \infty)$ and it maps onto the μ plane as shown in Fig. 8a; the other, defined by $(-2\pi \leq u \leq 0; -\infty < v < \infty)$ maps onto the μ plane as shown in Fig. 8b. In carrying out the transformation shown in Fig. 8a, the positive branch of $\mu = \sqrt{f(\xi) - f(\xi_s)}$ is used, whereas in carrying out the transformation shown in Fig. 8b, the negative branch of $\mu = \sqrt{f(\xi) - f(\xi_s)}$ is used.

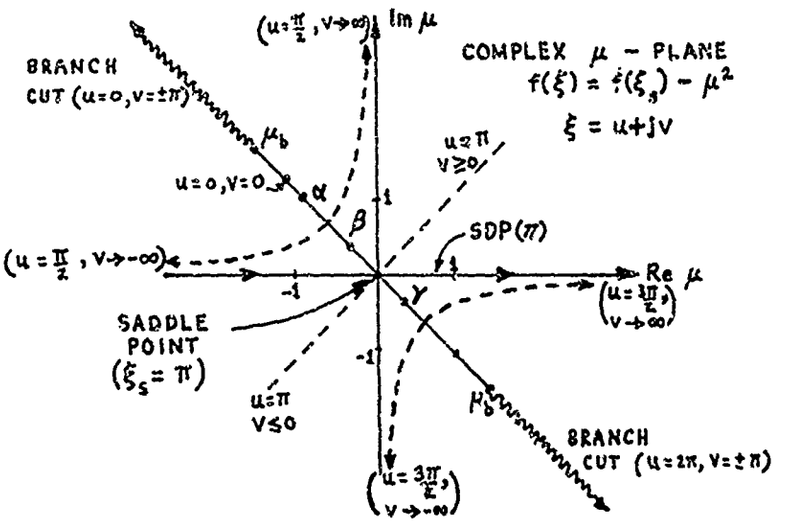

μ - PLANE REPRESENTATION FOR THE REGION CORRESPONDING TO $0 \le Re\,\xi \le 2\pi$ (SEE FIG.3)

FIG. 8a

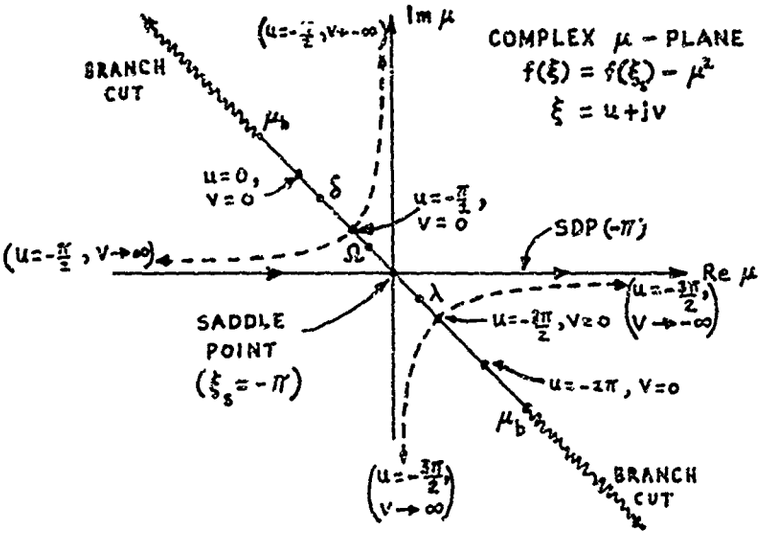

μ - PLANE REPRESENTATION FOR THE REGION CORRESPONDING TO $-2\pi \le Re\,\xi \le 0$ (SEE FIG.3)

FIG.8b

Fig. 8. Complex μ plane topology.

APPENDIX II

FIELD RELATIONS FOR SYSTEMS WITH NO VARIATION ALONG THE $\hat{z}$- (AXIAL) DIRECTION IN CYLINDRICAL COORDINATES

Let $\nabla = \nabla_t + \hat{z}\,\frac{\partial}{\partial z}$, where ∇_t is the component of the 3-D Laplacian operator ∇, which operates on the cylindrical coordinates transverse to $\hat{z}$.

Let $\bar{E} = \bar{E}_t + \bar{E}_z$ and $\bar{H} = \bar{H}_t + \bar{H}_z$, where $\bar{E}$ and $\bar{H}$ respectively are electric and magnetic field intensities satisfying Maxwell curl equations:

$$\text{(A-13)} \qquad \nabla \times \bar{E} = -j\omega\mu\,\bar{H} \text{ and } \nabla \times \bar{H} = j\omega\varepsilon\,\bar{E}.$$

$\bar{E}_t$ and $\bar{H}_t$ are the transverse (to z) field components and E_z, H_z are the axial fields (along $\hat{z}$).

For systems uniform in $\hat{z}$, one may separate out the z-dependence in $\bar{E}$ and $\bar{H}$ by assuming an $e^{-jk_z z}$ dependence. Next, equating the transverse components of the Maxwell curl equations gives:

$$\text{(A-14)} \qquad \begin{aligned} \nabla_t \times \bar{E}_z + \nabla_z \times \bar{E}_t &= -j\omega\mu\,\bar{H}_t \\ \nabla_t \times \bar{H}_z + \nabla_z \times \bar{H}_t &= j\omega\varepsilon\,\bar{E}_t \end{aligned}$$

(where $\nabla_z = \hat{z}\,\frac{\partial}{\partial z}$).

Finally, using the $e^{-jk_z z}$ dependence in $\bar{E}$ and $\bar{H}$ allows one to solve for $\bar{H}_t$ via (A-14) as follows

$$k^2\bar{H}_t = j\omega\varepsilon\,\nabla_t \times \bar{E}_z + \nabla_z \times \nabla_t \times \bar{H}_z + \nabla_z \times \nabla_z \times \bar{H}_t$$

or

$$k^2\bar{H}_t = j\omega\varepsilon\,\nabla_t \times \bar{E}_z - jk_z\,\nabla_t H_z + k_z^2\,\bar{H}_t$$

i.e.,

$$\text{(A-15)} \qquad \bar{H}_t = -jk_z \frac{\nabla_t H_z}{k^2 - k_z^2} + j\omega\varepsilon \frac{\nabla_t \times \bar{E}_z}{k^2 - k_z^2}$$

In a similar fashion, one may obtain:

$$\text{(A-16)} \qquad \bar{E}_t = -jk_z \frac{\nabla_t E_z}{k^2 - k_z^2} + j\omega\mu \frac{\hat{z} \times \nabla_t H_z}{k^2 - k_z^2}$$

(Note that $\nabla_t \times \bar{E}_z = -\hat{z} \times \nabla_t E_z$ in (A-15).)

Thus, (A-15) and (A-16) allow one to calculate $\bar{E}_t$ and $\bar{H}_t$ from a knowledge of E_z and H_z alone.

APPENDIX III

THE AXIAL FIELDS OF TRAVELING WAVE ELECTRIC AND MAGNETIC LINE SOURCES IN THE PRESENCE OF A PERFECTLY CONDUCTING INFINITE, 2-D WEDGE

Case 1 (Traveling wave electric current, $Ie^{-jk_z z'}$)

The magnetic vector potential $\bar{A}$ associated with the electric current $\hat{z}\, Ie^{-jk_z z'}$ satisfies:

(A-17) $\bar{A} = \hat{z}\, A_z$, and

$$(\nabla^2+k^2)A_z = -\mu \int_{-\infty}^{\infty} Ie^{-jk_z z'} \frac{\delta(\rho-\rho')\delta(\phi-\phi')\delta(z-z')}{\rho}\, dz' .$$

Let $A_z = a_z e^{-jk_z z}$ (since the source and the field A_z must have the same z-dependence for (A-17) to be true). Thus, (A-17) becomes

$$(A\text{-}18) \qquad \{\nabla_t^2 + (k^2-k_z^2)\}a_z = -\mu I \frac{\delta(\rho-\rho')\delta(\phi-\phi')}{\rho} .$$

Let

$$(A\text{-}19) \qquad k_t^2 = k^2 - k_z^2 .$$

The fields associated with A_z are given as:

$$(A\text{-}20) \qquad \bar{H} = \text{magnetic field intensity} = \frac{1}{\mu} \nabla \times \hat{z}\, A_z, \text{ and}$$

$$(A\text{-}21) \qquad \bar{E} = \text{electric field intensity} = -j\omega\, \hat{z}\, A_z + \frac{\nabla(\nabla \cdot A_z\hat{z})}{j\omega\mu\varepsilon}$$

The boundary conditions on A_z are the following:

(A-22) $E_\rho|_{\phi=0,n\pi} = 0$ implies $\frac{1}{j\omega\mu\epsilon} \frac{\partial^2}{\partial\rho} \frac{\partial A_z}{\partial z}\Big|_{\phi=0,n\pi} = 0,$

and

(A-23) $E_z|_{\phi=0,n\pi} = 0$ implies $j\omega A_z + \frac{1}{j\omega\mu\epsilon} \frac{\partial^2 A_z}{\partial z^2}\Big|_{\phi=0,n\pi} = 0$

For (A-22) and (A-23) to be simultaneously true, one gets

(A-24) $A_z|_{\phi=0,n\pi} = 0$

(and therefore $a_z|_{\phi=0,n\pi} = 0$).

In addition, A_z satisfies the radiation condition (for a time dependence of the type $e^{+j\omega t}$) and the Meixner edge condition. It follows that

(A-25) $a_z = \mu I\, G_s(\rho,\phi;\rho',\phi';k_t)$ where

$$(\nabla_t^2 + k_t^2)G_s(\rho,\phi;\rho',\phi';k_t) = -\frac{\delta(\rho-\rho')\delta(\phi-\phi')}{\rho}$$

and $G_s|_{\phi=0,n\pi} = 0$. Also G_s satisfies the radiation condition and the Meixner edge condition.

Finally,

$$E_z = \frac{1}{j\omega\mu\epsilon}\left(k^2 + \frac{\partial^2}{\partial z^2}\right) A_z = \frac{k_t^2}{j\omega\mu\epsilon} a_z e^{-jk_z z}, \quad H_z = 0;$$

or

(A-26) $E_z = \frac{k_t^2}{j\omega\epsilon} Ie^{-jk_z z} G_s(\rho,\phi;\rho',\phi';k_t), \quad H_z = 0.$

Case 2 (Traveling wave magnetic current, $Me^{-jk_z z'}$).

The vector electric potential $\bar{F}$ associated with the magnetic current $\hat{z}M\, e^{-jk_z z'}$ satisfies

(A-27) $\bar{F} = \hat{z}\, F_z$, and

$$(\nabla^2 + k^2)F_z = -\varepsilon \int_{-\infty}^{\infty} Me^{-jk_z z'} \frac{\delta(\rho-\rho')\delta(\phi-\phi')\ (z-z')}{\rho}\, dz'$$

Writing $F_z = f_z\, e^{-jk_z z}$ as before,

one obtains:

$$(A\text{-}28) \qquad (\nabla_t^2 + k_t^2)f_z = -\varepsilon M \frac{\delta(\rho-\rho')\delta(\phi-\phi')}{\rho} \quad .$$

Thus,

$$(A\text{-}29) \qquad f_z = -\varepsilon M\, G_h(\rho,\phi;\rho',\phi';k_t)$$

where

$$(A\text{-}30) \qquad (\nabla_t^2 + k_t^2)G_h(\rho,\phi;\rho',\phi';k_t) = -\frac{\delta(\rho-\rho')\delta(\phi-\phi')}{\rho} \quad .$$

The boundary conditions on F_z (and hence f_z) and G_h are identical and are obtained from

$$\left.\frac{\partial H_z}{\partial \phi}\right|_{\phi=0,n\pi} = 0 \quad \text{and} \quad \left.\frac{\partial H_\rho}{\partial \phi}\right|_{\phi=0,n\pi} = 0$$

where

$$\bar{H} = -j\omega \bar{F} + \frac{\nabla(\nabla \cdot \bar{F})}{j\omega\mu\varepsilon} \quad , \text{ and } \quad \bar{E} = -\frac{1}{\varepsilon} \nabla \times \bar{F}.$$

It follows that F_z, f_z and G_h satisfy:

$$\left.\frac{\partial G_h}{\partial \phi}\right|_{\phi=0,n\pi} = 0, \quad \left.\frac{\partial f_z}{\partial \phi}\right|_{\phi=0,n\pi} = 0 \quad \text{and} \quad \left.\frac{\partial F_z}{\partial \phi}\right|_{\phi=0,n\pi} = 0.$$

Finally the radiation condition and the Miexner edge conditions must also be satisfied. One may then write

(A-31) $$H_z = \frac{k_t^2}{j\omega\mu} M e^{-jk_z z} G_h(\rho,\phi;\rho',\phi';k_t), \qquad E_z = 0.$$

REFERENCES

1. Keller, J.B., "Geometrical Theory of Diffraction," Journal of the Optical Society of America, Vol. 52, February 1962, pp. 116-130.
2. Kouyoumjian, R.G., "Asymptotic High Frequency Methods," Proc. IEEE, Vol. 53, No. 8, August 1965, pp. 864-876.
3. Felsen, L.B., "Quasi Optic Diffraction," in Quasi-Optics, MRI Symposium Series, Vol. 14, Brooklyn, N.Y.: Polytechnic Press, Polytechnic Institute of Brooklyn, 1964, pp. 1-40.
4. MacDonald, H.M., Electric Waves, Cambridge: Cambridge Univ. Press, 1902; pp. 186-198.
5. Sommerfeld, A., "Asymptotische Darstellung von Formeln aus Beugungstheorie des Lichtes," J. reine u. angev. Math., Vol. 158 (1928), pp. 199-208.
6. Pauli, W., "On the Asymptotic Series for Functions in the Theory of the Diffraction of Light," Phys. Rev., Vol. 54, December 1938, pp. 924-931.
7. Oberhettinger, F., "On Asymptotic Series for Functions Occuring in the Theory of Diffraction of Waves by Wedges," J. Math. and Phys., Vol. 34, 1955, pp. 245-255.
8. Felsen, L.B. and Marcuvitz, N., "Modal Analysis and Synthesis of Electromagnetic Fields," Research Rept. No. PIB MRI-1083-62, Microwave Research Institute, Polytechnic Institue of Brooklyn, November 1962.

9. Hutchins, D.L. and Kouyoumjian, R.G., "Asymptotic Series Describing the Diffraction of a Plane Wave by a Wedge," Report 2183-3, ElectroScience Laboratory, Department of Electrical Engineering, The Ohio State University; prepared under Contract AF 19(628)-5929 for Air Force Cambridge Research Laboratories.

(see also: Hutchins, D.L. and Kouyoumjian, R.G., "A New Asymptotic Solution to the Diffraction by a Wedge," URSI Spring Meeting, Ottawa, Canada, May 1967.)

10. Nomura, Yukichi, "On the Complete Theory of Diffraction of Electric Waves by a Perfect Conducting Wedge," Science Reports of the Research Institutes, Tohoku University, Vol. 4, No. 1, December 1952.

11. Tuzhilin, A.A., "New Representations of Diffraction Fields in Wedge Shaped Regions with Ideal Boundaries," Soviet Physics - Acoustics, 9, 1963, pp. 168-172.

12. Tuzhilin, A.A., "Short-Wave Asymptotic Representation of Electromagnetic Diffraction Fields Produced by Arbitrarily Oriented Dipoles in a Wedge-Shaped Region with Ideally Conducting Sides," Annotation of Reports of the Third All-Union Symposium on Wave Diffraction, Acad. Sci. USSR, 1964, pp. 93-95.

13. Bowman, J.J. and Senior, T.B.A., "Diffraction of a Dipole Field by a Perfectly Conducting Half Plane," Radio Science, Vol. 2 (New Series), No. 11, November 1967, pp. 1339-1345.

14. Hutchins, D.L., "Asymptotic Series Describing the Diffraction of a Plane Wave by a Two-Dimensional Wedge of Arbitrary Angle," Ph.D. Dissertation, The Ohio State University, 1967.

15. Sommerfeld, A., Partial Differential Equations in Physics, New York: Academic Press, 1966.

16. Van Bladel, J., Electromagnetic Fields, New York: McGraw-Hill, 1966, pp. 382-393.

17. Kouyoumjian, R.G., unpublished lecture notes for Advanced Courses in Electromagnetic Theory given in the Department of Electrical Engineering at The Ohio State University, Columbus, Ohio.

18. Tsai, L.L. and Rudduck, R.C., "Accuracy of Approximate Formulations for Near-Field Wedge Diffraction of a Line Source," Report 1691-18, ElectroScience Laboratory (formerly Antenna Laboratory), Department of Electrical Engineering, The Ohio State University; prepared under Grant Number NsG-448 for National Aeronautics and Space Administration.

19. Harrington, R.F., Time Harmonic Electromagnetic Fields, New York: McGraw-Hill, 1961, Chapters V and VI.

20. Keller, J.B., "Diffraction by an Aperture, Journal of Applied Physics, Vol. 28, April 1957, pp. 426-444.

21. Kouyoumjian, R.G., "A Note on the Caustic Associated with Edge Diffraction," to be submitted for publication.

UNCLASSIFIED

Security Classification

DOCUMENT CONTROL DATA - R&D

(Security classification of title, body of abstract and indexing annotation must be entered when the overall report is classified)

1. ORIGINATING ACTIVITY *(Corporate author)*: ElectroScience Laboratory, Department of Electrical Engineering, The Ohio State University Research Foundation, Columbus, Ohio 43212

2a. REPORT SECURITY CLASSIFICATION: Unclassified

2b. GROUP:

3. REPORT TITLE: THE DYADIC DIFFRACTION COEFFICIENT FOR A PERFECTLY CONDUCTING WEDGE

4. DESCRIPTIVE NOTES *(Type of report and inclusive dates)*: Scientific. Interim

5. AUTHOR(S) *(Last name, first name, initial)*:
P. H. Pathak
R. G. Kouyoumjian

6. REPORT DATE: 5 June 1970

7a. TOTAL NO. OF PAGES: 87

7b. NO. OF REFS: 21

8a. CONTRACT OR GRANT NO.: Contract AF 19(628)-5929

b. Project, Task, Work Unit Nos. 5635-02-01

c. DoD Element 6144501F

d. DoD Subelement 681305

9a. ORIGINATOR'S REPORT NUMBER(S): ElectroScience Laboratory 2183-4

9b. OTHER REPORT NO(S) *(Any other numbers that may be assigned this report)*: AFCRL-69-0546

10. AVAILABILITY/LIMITATION NOTICES: This document has been approved for public release and sale; its distribution is unlimited.

11. SUPPLEMENTARY NOTES: TECH, OTHER

12. SPONSORING MILITARY ACTIVITY: Air Force Cambridge Research Laboratories (CRD) L.G. Hanscom Field Bedford, Massachusetts 01730

13. ABSTRACT

A ray-fixed coordinate system is introduced and used to derive a new, compact form of the dyadic diffraction coefficient for an electromagnetic wave incident on a perfectly-conducting wedge. This diffraction coefficient is merely the sum of two dyads; furthermore, with the use of simple correction factors which have the same form for plane, cylindrical, conical or spherical waves incident on the edge, the dyadic diffraction coefficient is valid in the transition regions of the shadow and reflection boundaries.

DD FORM 1 JAN 64 1473

UNCLASSIFIED

Security Classification

14. KEY WORDS	LINK A		LINK B		LINK C	
	ROLE	WT	ROLE	WT	ROLE	WT
Electromagnetic wedge diffraction Dyadic diffraction coefficient Transition regions Plane wave illumination Cylindrical wave illumination Spherical wave illumination Conical wave illumination Green's function						

INSTRUCTIONS

1. ORIGINATING ACTIVITY. Enter the name and address of the contractor, subcontractor, grantee, Department of Defense activity or other organization *(corporate author)* issuing the report.

2*a*. REPORT SECURITY CLASSIFICATION. Enter the overall security classification of the report. Indicate whether "Restricted Data" is included. Marking is to be in accordance with appropriate security regulations.

2*b*. GROUP. Automatic downgrading is specified in DoD Directive 5200.10 and Armed Forces Industrial Manual. Enter the group number. Also, when applicable, show that optional markings have been used for Group 3 and Group 4 as authorized.

3. REPORT TITLE: Enter the complete report title in all capital letters. Titles in all cases should be unclassified. If a meaningful title cannot be selected without classification, show title classification in all capitals in parenthesis immediately following the title.

4. DESCRIPTIVE NOTES: If appropriate, enter the type of report, e.g., interim, progress, summary, annual, or final. Give the inclusive dates when a specific reporting period is covered.

5. AUTHOR(S): Enter the name(s) of author(s) as shown on or in the report. Enter last name, first name, middle initial. If military, show rank and branch of service. The name of the principal author is an absolute minimum requirement.

6. REPORT DATE: Enter the date of the report as day, month, year, or month, year. If more than one date appears on the report, use date of publication.

7*a*. TOTAL NUMBER OF PAGES: The total page count should follow normal pagination procedures, i.e., enter the number of pages containing information.

7*b*. NUMBER OF REFERENCES: Enter the total number of references cited in the report.

8*a*. CONTRACT OR GRANT NUMBER. If appropriate, enter the applicable number of the contract or grant under which the report was written.

8*b*, 8*c*, & 8*d*. PROJECT NUMBER: Enter the appropriate military department identification, such as project number, subproject number, system numbers, task number, etc.

9*a*. ORIGINATOR'S REPORT NUMBER(S). Enter the official report number by which the document will be identified and controlled by the originating activity. This number must be unique to this report.

9*b*. OTHER REPORT NUMBER(S): If the report has been assigned any other report numbers *(either by the originator or by the sponsor)*, also enter this number(s).

10. AVAILABILITY/LIMITATION NOTICES: Enter any limitations on further dissemination of the report, other than those imposed by security classification, using standard statements such as:

(1) "Qualified requesters may obtain copies of this report from DDC."

(2) "Foreign announcement and dissemination of this report by DDC is not authorized."

(3) "U. S. Government agencies may obtain copies of this report directly from DDC. Other qualified DDC users shall request through

_____."

(4) "U. S. military agencies may obtain copies of this report directly from DDC. Other qualified users shall request through

_____"

(5) "All distribution of this report is controlled. Qualified DDC users shall request through

_____."

If the report has been furnished to the Office of Technical Services, Department of Commerce, for sale to the public, indicate this fact and enter the price, if known.

11. SUPPLEMENTARY NOTES: Use for additional explanatory notes.

12. SPONSORING MILITARY ACTIVITY: Enter the name of the departmental project office or laboratory sponsoring *(paying for)* the research and development. Include address.

13. ABSTRACT: Enter an abstract giving a brief and factual summary of the document indicative of the report, even though it may also appear elsewhere in the body of the technical report. If additional space is required, a continuation sheet shall be attached.

It is highly desirable that the abstract of classified reports be unclassified. Each paragraph of the abstract shall end with an indication of the military security classification of the information in the paragraph, represented as *(TS)*, *(S)*, *(C)*, or *(U)*.

There is no limitation on the length of the abstract. However, the suggested length is from 150 to 225 words.

14. KEY WORDS. Key words are technically meaningful terms or short phrases that characterize a report and may be used as index entries for cataloging the report. Key words must be selected so that no security classification is required. Identifiers, such as equipment model designation, trade name, military project code name, geographic location, may be used as key words but will be followed by an indication of technical context. The assignment of links, rules, and weights is optional.